

Table 1 Patient background

Parameter	Total (%) <i>n</i> = 60	Responders (%) <i>n</i> = 47	Non-responders (%) <i>n</i> = 13	<i>P</i> value
Age (median, years)	68 (45–82)	68 (45–82)	68 (51–79)	0.693
Gender				
Male	45 (75)	36 (76.6)	9 (69.2)	0.587
Female	15 (25)	11 (24.4)	4 (30.8)	
Small cell carcinoma	29 (48.3)	22 (46.8)	7 (53.8)	0.807
Non-small cell carcinoma	31 (51.7)	22 (53.2)	6 (46.2)	
Chronic obstructive pulmonary disease (COPD)				
+	38 (63.3)	31 (63.3)	7 (53.8)	0.117
–	22 (36.7)	16 (26.7)	6 (46.2)	
Multinational Association of Supportive Care in Cancer (MASCC) score				
<21	20 (33.3)	15 (31.9)	5 (38.5)	0.653
≥21	40 (66.6)	32 (68.1)	8 (61.5)	
Chemotherapy				0.255
Single agent	21 (35.0)	14 (29.8)	7 (53.8)	
Platinum-based regimen	38 (63.3)	32 (68.1)	6 (46.2)	
Other	1 (1.7)	1 (2.1)	0 (0.0)	
Number of chemotherapy cycles given before febrile neutropenia (FN)				0.741
1	28 (46.7)	23 (48.9)	5 (38.5)	
2	9 (15.0)	6 (12.8)	3 (23.0)	
3	1 (1.7)	1 (2.1)	0 (0.0)	
>4	22 (36.7)	17 (36.2)	5 (38.5)	
Antimicrobial agents				0.222
Cephalosporin	26 (43.3)	21 (44.7)	5 (38.5)	
Carbapenem	19 (31.7)	14 (29.8)	5 (38.5)	
Fluoroquinolone	14 (23.3)	12 (25.5)	2 (15.3)	
Carbapenem + fluoroquinolone	1 (1.7)	0 (0.0)	1 (7.7)	

Table 2 Parameters at onset of febrile neutropenia (FN)

Parameter	Total	Responders	Non-responders	<i>P</i> value
Temperature (°C)	38.3 (0.06)	38.2 (0.07)	38.2 (0.17)	0.278
MASCC score	22.4 (0.4)	22.6 (0.4)	21.4 (0.8)	0.187
WBC (/ μ l)	1323 (48)	1404 (42)	1030 (72)	0.062
Neutrophils (/ μ l)	307 (40)	347 (45)	163 (77)	0.056
TP (mg/dl)	6.7 (0.1)	6.8 (0.1)	6.4 (0.3)	0.073
Alb (mg/dl)	3.3 (0.07)	3.3 (0.07)	3.1 (0.17)	0.096
AST (IU/l)	22 (2.5)	23.3 (3.2)	18.6 (1.7)	0.428
LDH (IU/l)	256 (70)	287 (92)	168 (14)	0.178
ALP (IU/l)	303 (59)	325 (74)	233 (32)	0.510
BUN (mg/dl)	18.2 (1.8)	16.6 (1.3)	23.7 (6.8)	0.106
CRP (mg/dl)	7.0 (1.0)	5.7 (1.1)	11.5 (2.1)	0.016

Data are presented as mean \pm standard error

WBC white blood cells, TP total protein, Alb albumin, AST aspartate amino transferase, ALT alanine aminotransferase, LDA lactate dehydrogenase, ALP alkaline phosphatase, BUN blood urea nitrogen, CRP C-reactive protein

However, there were no significant differences in body temperature, MASCC score, white blood cell counts, and neutrophil counts.

Parameters with $P < 0.20$ as determined by a single logistic regression analysis were adopted as candidates for the multiple logistic analysis. The most appropriate model

Table 3 Results of multiple logistic analysis of patient characteristics as continuous variables and treatment failure

Parameter	Odds ratio	95 % confidence interval (CI)	P value
CRP (>10 mg/dl)	11.0	1.635–74.5	0.014
TP (mg/dl)	0.32	0.081–1.30	0.112
Alb (mg/dl)	2.40	0.306–18.9	0.405
WBC (/ μ l)	1.05	0.906–1.22	0.513
Neutrophils (/ μ l)	0.765	0.548–1.07	0.115

Table 4 Modified MASCC score for predicting non-responders to initial antimicrobial agents

Characteristic	Score
Febrile neutropenia (FN) with no or mild symptoms	5
No hypotension (systolic blood pressure >90 mmHg)	5
No chronic obstructive pulmonary disease (COPD)	4
Solid tumor or hematological malignancy with no previous fungal infection	4
No dehydration requiring parenteral fluids	3
Febrile neutropenia with moderate symptoms	3
Outpatient status	3
Age <60 years	2
Serum CRP at the time of FN onset <10 mg/dl	3

A score of <22 predicted a non-responder status

was selected with a stepwise method. The parameters described below were selected as independent risk factors of treatment failure. The elevation of the serum CRP level at the time of FN onset was a strong independent risk factor for the failure of initial treatment. The multivariate analysis demonstrated that a CRP level higher than 10 mg/dl is an independent risk factor for the failure of initial antimicrobial agents for febrile neutropenia with lung cancer (OR 11.0, 95 % CI 1.635–74.5) (Table 3).

As the next step, we tried to confirm whether a serum CRP level higher than 10 mg/dl predicts the failure of initial antimicrobial agents. The MASCC score demonstrated that the sensitivity of the prediction of failure of the initial antimicrobial agents used for FN was 0.695, specificity was 0.385, positive predictive value (PPV) was 0.800, and negative predictive value (NPV) was 0.26. The MASCC score did not show a good predictive value, so we added the CRP level to the MASCC score as a new item. We added three points to the MASCC score for patients with a serum CRP level less than 10 mg/dl, and the cutoff value was set to 22 (Table 4). As a result, the modified MASCC score improved the results, and the sensitivity of the prediction of failure of the initial antimicrobial agents used for FN was 0.870, specificity was 0.462, PPV was 0.851, and NPV was 0.50 (Table 5).

Table 5 Results of modified MASCC score for sensitivity of predicting treatment failure for initial antimicrobial agents

Parameter	MASCC	Modified MASCC
Sensitivity	0.695	0.870
Specificity	0.385	0.462
PPV	0.800	0.851
NPV	0.26	0.50

We added three points to the MASCC score for patients with a serum CRP level less than 10 mg/dl, and the cutoff value was set at 22 (modified MASCC score), as shown in Table 4

PPV positive predictive value, NPV negative predictive value

Discussion

In the present study, predictive factors for the failure of initial antimicrobial agents for the treatment of FN in patients with lung cancer were analyzed. Elevation of serum CRP level at the time of FN onset could be a candidate predictive factor for the failure of treatment on the basis of a simple logistic regression analysis and a multivariate analysis. In this study, the cutoff value for the serum CRP level was determined to be 11.3 mg/dl. A multivariate analysis demonstrated a CRP level higher than 11.3 mg/dl to be an independent risk factor for the failure of initial antimicrobial agents for FN with lung cancer (OR 11.2, 95 % CI 1.64–75.9). As Chalmers et al. [10] demonstrated low CRP levels (<10 mg/dl) on admission to be independently associated with a reduced 30-day mortality, the cutoff value for the serum CRP level was set to 10 mg/dl. The odds ratio of the serum CRP level at 11.3 mg/dl was the same as that for 10 mg/dl. We therefore determined a serum CRP level of 10 mg/dl to be a strong predictive factor for treatment failure.

C-reactive protein was originally discovered by Tillet and Francis [11] in 1930 as a substance present in the serum of patients with acute inflammation that reacted with the C polysaccharide of pneumococci. CRP has been used for diagnosing infectious diseases and as a marker for the assessment of treatment. However, patients with lung cancer often show elevated CRP levels even in the absence of an infectious disease. Cancer itself can induce inflammation, which results in increase in CRP [12, 13]. Another issue is that the elevation of CRP is not always associated with the prognosis of the disease. In the case of community-acquired pneumonia, neither the IDSA/American Thoracic Society consensus guidelines [14] nor the British Thoracic Society guidelines [15] describe that serum CRP is an index of the severity of the pneumonia. However, Chalmers et al. [10] documented that low CRP levels (<10 mg/dl) on admission were independently associated with a reduced 30-day mortality (OR 0.18, 95 % CI

0.04–0.85). The guidelines for Japanese hospital-acquired pneumonia state that patients who showed a serum CRP level greater than 20 mg/dl had a higher mortality rate [16]. In a previous report, we demonstrated that the severity of FN and the serum CRP level were risk factors for refractory FN in patients with lung cancer [9]. However, Bajwa and colleagues [17] have reported that the plasma levels of CRP within 48 h of acute respiratory distress syndrome (ARDS) onset are associated with improved survival. In the present study, we demonstrated results similar to those previously reported by Fujita et al. [9]. Taking these references into consideration, we hypothesized that the serum CRP level at the onset of FN could be important for predicting the response, and that the CRP level in the FN patients is associated with the severity of infection.

Actually, the MASCC score has been proposed for the selection of low-risk patients but not for predicting the failure of initial antimicrobial agents in FN. In this study, we wondered whether the MASCC score per se could predict the response of FN patients with lung cancer to the initial antimicrobial agents. In the present study, the MASCC score did not indicate the response. However, when the CRP score was added to the MASCC score, the new score could predict the failure of initial antimicrobial agents in FN patients with lung cancer more precisely than the classic MASCC score. We also investigated how much weight should be assigned to the CRP level to most accurately serve as a predictor of the response. Three points were deemed to be the most appropriate, rather than one, two, or five points (data not shown). To predict the failure of initial antimicrobial agents used to treat FN patients with lung cancer, the CRP score should be added to the MASCC score. Because the present study was a retrospective study, further studies are needed to confirm the present conclusions.

Another issue is what antimicrobial agents should be used if the modified MASCC score predicts the failure of the conventional agents. At the present time, this issue remains controversial. Fleischhack and colleagues [18] reported that the success rate of initial monotherapy with meropenem was more effective than that with cefetazidime. However, there was a report that monotherapy with cefepime demonstrated a high degree of clinical efficacy and safety in the treatment of FN in patients with lung cancer [19]. As shown in Table 1, FN is treated with carbapenem at a high frequency (31.7 %) in the present study. Some researchers have been concerned that the use of carbapenem more than 7 days could lead to the emergence of multidrug-resistant *Pseudomonas aeruginosa* [20]. The American Thoracic Society and Infectious Diseases Society of America guidelines recommend that hospital-acquired pneumonia should be treated with early, appropriate, broad-spectrum, combination therapy [21].

However, this treatment has also been reported to lead to both increased mortality and renal dysfunction [22]. The issue concerning the selection of microbial agents needs to be resolved in the near future.

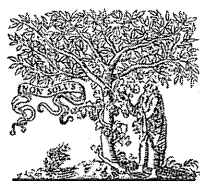
Acknowledgments We appreciate the assistance of Dr. Brian Quinn for editing the manuscript and ensuring correct English usage.

Conflict of interest None.

References

- Kuderer NM, Dale DC, Crawford J, Cosler LE, Lyman GH. Mortality, morbidity and cost associated with febrile neutropenia in adult cancer patients. *Cancer (Phila)*. 2006;106:2258–66.
- Hughes WT, Armstrong D, Bodey GP, Feld R, Mandell GL, Meyers JD, et al. From the Infectious Diseases Society of America guidelines for the use of antimicrobial agents in neutropenic patients with unexplained fever. *J Infect Dis*. 1990;161:381–96.
- Hughes WT, Armstrong D, Bodey GP, Brown AE, Edwards JE, Feld R, et al. 1997 guidelines for the use of antimicrobial agents in neutropenic patients with unexplained fever. *Clin Infect Dis*. 1997;25:551–73.
- Hughes WT, Armstrong D, Bodey GP, Bow EJ, Brown AE, Calandra T, et al. 2002 guidelines for the use of antimicrobial agents in neutropenic patients with cancer. *Clin Infect Dis*. 2002;34:730–51.
- Freifeld AG, Bow EJ, Sepkowitz KA, Boeckh MJ, Ito JI, Mullen CA, et al. Clinical practice guideline for the use of antimicrobial agents in neutropenic patients with cancer: 2010 update by the Infectious Diseases Society of America. *Clin Infect Dis*. 2011; 52:e56–93.
- Masaoka T. Conclusions and recommendations: evidence-based recommendations on antimicrobial use in febrile neutropenia in Japan. *Int J Hematol*. 1998;68:S5–6.
- Masaoka T. Evidence-based recommendations for antimicrobial use in febrile neutropenia in Japan: executive summary. *Clin Infect Dis*. 2004;39:S49–52.
- Klastersky J, Paesmans M, Ruvbenstein EB, Bover M, Elting L, Feld R, et al. The multinational association for supportive care in cancer risk index: a multinational scoring system for identifying low-risk febrile neutropenic cancer patients. *J Clin Oncol*. 2000; 16:3038–51.
- Fujita M, Tokunaga S, Ikegame S, Harada E, Matsumoto T, Uchino J, et al. Identifying risk factors for refractory febrile neutropenia in patients with lung cancer. *J Infect Chemother*. 2012;18:53–8.
- Chalmers JD, Singanayagam A, Hill AT. C-reactive protein is an independent predictor of severity in community-acquired pneumonia. *Am J Med*. 2008;121:219–25.
- Tillett WS, Francis T. Serological reactions in pneumonia with a nonprotein somatic fraction of pneumococcus. *J Exp Med*. 1930;53:561–71.
- Grivennikov SI, Greten FR, Karin M. Immunity, inflammation, and cancer. *Cell*. 2010;140:883–9.
- Slatore CG, Au DH, Littman AJ, Satia JA, White E. Association of nonsteroidal anti-inflammatory drugs with lung cancer: result from a large cohort study. *Cancer Epidemiol Biomarkers Prev*. 2009;18:1203–7.
- Mandell LA, Wunderink RG, Anzueto A, Bartlett JG, Campbell GD, Dean NC, et al. Infectious Diseases Society of America/American Thoracic Society consensus guideline on the management of

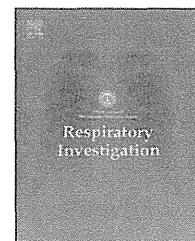
- community-acquired pneumonia in adults. *Clin Infect Dis*. 2007;44:s27–72.
15. Neill AM, Martin IR, Weir R, Anderson R, Cheresky A, Epton MJ, et al. Community acquired pneumonia: aetiology and usefulness of severity criteria on admission. *Thorax*. 1996;51: 1010–6.
 16. The committee for the Japanese Respiratory Society guidelines in the management of Respiratory Infections. The Japanese Respiratory Society guidelines for the management of hospital-acquired pneumonia in adults 2008. *Respirology*. 2009;14:S1–71.
 17. Bajwa EK, Khan UA, Januzzi JL, Gong MN, Thompson BT, Christiani DC. Plasma C-reactive protein levels are associated with improved outcome in ARDS. *Chest*. 2009;136:471–80.
 18. Fleischhack G, Hartmann C, Simon A, Wulff B, Havers W, Marklein G, et al. Meropenem versus ceftazidime as empirical monotherapy in febrile neutropenia of paediatric patients with cancer. *J Antimicrob Chemother*. 2001;47:841–53.
 19. Fujita M, Ouchi H, Inoue Y, Inoshima I, Ohshima T, Yoshimura C, et al. Clinical efficacy and safety of cefepime in febrile neutropenic patients with lung cancer. *J Infect Chemother*. 2010;16: 113–7.
 20. Ohmagari N, Graviss H, Graviss L, Hackett B, Perego C, Gonzalez V, et al. Risk factors for infections with multidrug-resistant *Pseudomonas aeruginosa* in patients with cancer. *Cancer (Phila)*. 2005;104:205–12.
 21. American Thoracic Society and the Infectious Diseases Society of America. Guidelines for the management of adults with hospital-acquired, ventilator-associated, and healthcare-associated pneumonia. *Am J Respir Crit Care Med*. 2005;171:388–416.
 22. Kett DH, Cano E, Quartin AA, Mangino J, Zervos MJ, Peyrani P, et al. Implementation of guideline for management of possible multidrug-resistant pneumonia in intensive care: an observational, multicentre cohort study. *Lancet Infect Dis*. 2011;11:181–9.



ELSEVIER

Contents lists available at ScienceDirect

Respiratory Investigation

journal homepage: www.elsevier.com/locate/resinv

Original article

A nationwide epidemiological survey of chronic hypersensitivity pneumonitis in Japan



Tsukasa Okamoto^{a,*}, Yasunari Miyazaki^a, Takashi Ogura^b, Kingo Chida^c, Nobuoki Kohno^d, Shigeru Kohno^e, Hiroyuki Taniguchi^f, Shinobu Akagawa^g, Yoshiro Mochizuki^h, Kohei Yamauchiⁱ, Hiroki Takahashi^j, Takeshi Johkoh^k, Sakae Homma^l, Kazuma Kishi^m, Soichiro Ikushimaⁿ, Satoshi Konno^o, Michiaki Mishima^p, Ken Ohta^q, Yasuhiko Nishioka^r, Nobuyuki Yoshimura^s, Mitsuru Munakata^t, Kentaro Watanabe^u, Yoshihiro Miyashita^v, Naohiko Inase^a

ARTICLE INFO

Article history:

Received 15 January 2013

Received in revised form

25 March 2013

Accepted 26 March 2013

Available online 6 June 2013

Keywords:

Hypersensitivity pneumonitis

Extrinsic allergic alveolitis

Pulmonary fibrosis

Surveillance

ABSTRACT

Background: In 1999, a Japanese epidemiological survey of chronic hypersensitivity pneumonitis (HP) showed that summer-type HP was the most prevalent variant of the disease. The number of reported cases of chronic HP has recently been increasing, and the clinical features of the disease seem to have changed. We conducted another nationwide epidemiological survey of chronic HP in Japan to determine better estimates of the frequency and clinical features of the disease.

Methods: A questionnaire was sent to qualified hospitals throughout Japan, and data on cases of chronic HP diagnosed between 2000 and 2009 were collected.

Results: In total, 222 cases of chronic HP from 22 hospitals were studied. Disease subtypes included bird-related HP ($n=134$), summer-type HP ($n=33$), home-related HP ($n=25$), farmer's lung ($n=4$), isocyanate-induced HP ($n=3$), and other types ($n=23$). The median proportion of lymphocytes in bronchoalveolar lavage fluid was high (24.5%). The primary findings of computed tomography of the chest were ground-glass attenuation and interlobular septal thickening. Centrilobular fibrosis was the major pathological finding on examination of surgical lung biopsy specimens from 93 patients. The median survival time was 83 months.

Conclusions: The proportion of bird-related HP was higher than that in the previous epidemiological survey, and the proportions of isocyanate-induced HP and farmer's lung were lower. A crucial step in diagnosing chronic HP is to thoroughly explore the possibility of antigen exposure.

© 2013 The Japanese Respiratory Society. Published by Elsevier B.V. All rights reserved.

^aDepartment of Integrated Pulmonology, Tokyo Medical and Dental University, 1-5-45, Yushima, Bunkyo-ku, Tokyo 113-8519, Japan

^bDepartment of Respiratory Medicine, Kanagawa Cardiovascular and Respiratory Center, 6-16-1, Tomiokahigashi, Kanagawa-ku, Yokohama City, Kanagawa 236-0051, Japan

^cDepartment of Respiratory Medicine, Hamamatsu University School of Medicine, 1-20-1, Handayama, Higashi-ku, Hamamatsu City, Shizuoka 431-3192, Japan

^dDepartment of Molecular and Internal Medicine, Hiroshima University, 1-2-3, Kasumi, Minami-ku, Hiroshima City, Hiroshima 734-8551, Japan

*Corresponding author. Tel.: +81 3 5803 5954; fax: +81 3 5803 0260.

E-mail address: "scrap_string"tokamoto.pulm@tmd.ac.jp (T. Okamoto).

1. Introduction

Hypersensitivity pneumonitis (HP) is an immunologically mediated lung disease induced by inhalation of antigens contained in a variety of organic dusts. HP is usually classified into acute, subacute, and chronic forms, although the subacute form might be a variant of acute HP [1]. Chronic HP is thought to be influenced by persistent or recurrent exposure to an antigen. Potential sources of inciting antigen vary among geographic regions and are influenced by multiple climatic, cultural, socioeconomic, and occupational factors. The clinical manifestations are heterogeneous and are likely to be determined by the intensity and frequency of exposure to etiologic antigens, as well as by genetic susceptibility [2]. The clinical features of chronic HP, namely, the physical findings, radiological and pathological abnormalities, and poor prognosis, are similar to those of idiopathic pulmonary fibrosis (IPF) [3].

A nationwide epidemiological survey of chronic HP in Japan was reported in 1999 [4]. The report covered 36 cases of chronic HP, including summer-type HP ($n=10$), bird fancier's lung (BFL, $n=7$), home-related HP ($n=5$), isocyanate-induced HP ($n=5$), farmer's lung ($n=4$), and other variants of the disease ($n=5$). Among the forms of acute HP in Japan, summer type was reported to be the most prevalent (81.9% of 331 cases) and BFL accounted for only 5.7% of cases [5]. Pulmonary physicians, radiologists, and pathologists now take steps to differentiate chronic HP from IPF. An important step in discriminating chronic HP from IPF/unusual interstitial pneumonia is to thoroughly explore the possibility of antigen exposure, because avoidance of antigen exposure may improve a patient's condition or halt disease progression. Since the last epidemiological survey was conducted, the number of reported cases of chronic HP has been increasing and the clinical characteristics of the disease seem to have changed.

Our group conducted another nationwide epidemiological survey of chronic HP in Japan to determine better estimates of the frequency and clinical characteristics of the disease over the past decade.

2. Materials and methods

2.1. Patient selection

The Research Committee on Diffuse Lung Diseases, a study group organized and sanctioned by the Japanese Ministry of Health, Labour and Welfare, conducted a survey on the status of chronic HP from 2000 to 2009. The committee sent a questionnaire to 25 qualified hospitals throughout Japan; data on 253 cases were collected from 22 hospitals, and data on 222 patients who satisfied the diagnostic criteria for chronic HP [4,6] were collected from the questionnaires. The diagnostic criteria for chronic HP included clinical improvement after withdrawal from the suspected environment and/or reproduction of symptoms by an environmental provocation or laboratory-controlled inhalation of a causative antigen and/or antibodies or lymphocyte proliferation to the presumptive antigen, evidence of pulmonary fibrosis on a pathological examination or on computed tomography (CT) scans, and respiratory symptoms related to HP for 6 months or longer [4].

2.2. Questionnaire

The questionnaire survey covered the following topics: causative antigens, symptoms, physical findings, laboratory findings, pulmonary function tests, bronchoalveolar lavage (BAL), radiography and CT findings, pathological findings of surgical lung biopsy specimens, immunological findings on specific antibodies, the lymphocyte proliferation test [7], the provocation test [8], treatment, and prognosis. Data on each patient were described by members of the Research Committee or by members of the Japan Respiratory Society serving as staff at the hospitals that returned the questionnaires. The study conformed to the Declaration of Helsinki and was approved by the internal review board of every institution that responded. Approval was obtained from the institutional review board on April 12, 2012, and the approval number was 1040.

^eSecond Department of Internal Medicine, Nagasaki University, 1-7-1, Sakamoto, Nagasaki City, Nagasaki 852-8501, Japan

^fDepartment of Respiratory Medicine and Allergy, Tosei General Hospital, 160-Banchi, Nishioiwake, Seto City, Aichi 489-8642, Japan

^gDepartment of Respiratory Medicine, National Hospital Organization, Tokyo National Hospital, 3-1-1, Takeoka, Kiyose City, Tokyo 204-8585, Japan

^hDepartment of Internal Medicine, Himeji Medical Center, 68-Banchi, Honnmachi, Himeji City, Hyogo 670-8520, Japan

ⁱDepartment of Internal Medicine, Iwate Medical University, 19-1, Maruuchi, Morioka City, Iwate 020-8505, Japan

^jDepartment of Internal Medicine, Sapporo Medical University, 16-291, Minamiichijo-nishi, Chuo-ku, Sapporo City, Hokkaido 060-8543, Japan

^kDepartment of Radiology, Kinki Central Hospital, 3-1, Kurumazuka, Itami City, Hyogo 664-8533, Japan

^lDepartment of Respiratory Medicine, Toho University, 6-11-1, Omori-nishi, Ota-ku, Tokyo 143-8541, Japan

^mDepartment of Respiratory Medicine, Toranomon Hospital, 2-2-2, Toranomon, Minato-ku, Tokyo 105-8470, Japan

ⁿDepartment of Respiratory Medicine, Japanese Red Cross Medical Center, 4-1-22, Hiroo, Shibuya-ku, Tokyo 150-8935, Japan

^oFirst Department of Medicine, Hokkaido University, 5-chome, Kita14-Jo-Nishi, Kita-ku, Sapporo City, Hokkaido 060-8648, Japan

^pDepartment of Respiratory Medicine, Kyoto University, 54-banchi, Kawara-cho, Seigoinn, Sakyo-ku, Kyoto City, Kyoto 606-8507, Japan

^qDepartment of Internal Medicine, Teikyo University, 2-11-1, Kaga, Itabashi-ku, Tokyo 173-0003, Japan

^rDepartment of Respiratory Medicine, Tokushima University, 2-50-1, Kuramoto-cho, Tokushima City, Tokushima 770-8503, Japan

^sDepartment of Respiratory Medicine, Hiratsuka Kyosai Hospital, 9-11, Oiwake, Hiratsuka City, Kanagawa 254-8502, Japan

^tDepartment of Pulmonary Medicine, Fukushima Medical University, 1-banchi, Hikarigaoka, Fukushima City, Fukushima 960-1295, Japan

^uDepartment of Respiratory Medicine, Fukuoka University, 7-45-1, Nanakuma, Jonan-ku, Fukuoka City, Fukuoka 814-0180, Japan

^vDepartment of Respiratory Medicine, Yamanashi Prefectural Central Hospital, 1-1-1, Fujimi, Kofu City, Yamanashi 400-8506, Japan

2.3. Statistical analysis

Data were analyzed using Prism 5 (GraphPad Software, Inc., San Diego, CA) and are expressed as medians and 25th-75th percentiles. Comparisons between groups were performed using one-way analysis of variance for continuous variables and the χ^2 or Fisher's exact test for categorical variables. The log-rank test was used to compare survival between the patients in each group. Correlation coefficients were obtained using the Spearman's correlation coefficient test. All statistical comparisons were 2-sided, and *p* values less than 0.05 were considered statistically significant.

3. Results

3.1. Characteristics of each HP group

The 222 cases of chronic HP analyzed in the study included the following variants of the disease: bird-related HP (*n*=134), summer-type HP (*n*=33), home-related HP (*n*=25), farmer's lung (*n*=4), isocyanate-induced HP (*n*=3), and other types (*n*=23) (Table 1). The other types of chronic HP consisted of 19 cases with unknown causative antigen, 2 cases of hot tub lung, 1 case induced by organic manure, and 1 case induced by wood debris. We recognized bird-related HP in all areas of Japan. However, there were few cases of summer-type HP and home-related HP in northern areas of the country (A and B), and farmer's lung was identified in the agricultural area (Fig. 1). The median age at diagnosis was 64.0 years. A predominance of male patients had summer-type HP, home-related HP, isocyanate-induced HP, and farmer's lung. A female predominance was observed in only 1 subgroup: bird-related HP. One-half of the patients (52.8%) with chronic HP had a history of smoking. The median duration from onset of HP-associated respiratory symptoms to the first hospital visit was 15.0 months. The median observation period was 31.0 months.

3.2. Symptoms and physical findings

The primary symptoms of chronic HP were cough (73.3%) and dyspnea on exertion (72.7%). Sputum was observed in 30.7% of the cases, and fever was seen in only 16.1% (Table 2). Slightly more than one-tenth of the cases (11.9%) were asymptomatic. Fine crackles and clubbed fingers were observed in 91.4% and 32.7% of the cases, respectively.

3.3. Laboratory data

The median white blood cell count and median level of C-reactive protein were within normal limits (Table 3). The median values of Krebs von den Lungen 6 (KL-6) and surfactant protein D (SP-D), 2 established markers of pulmonary fibrosis, were abnormally high (1448 U/mL and 240 ng/mL, respectively). Anti-nuclear

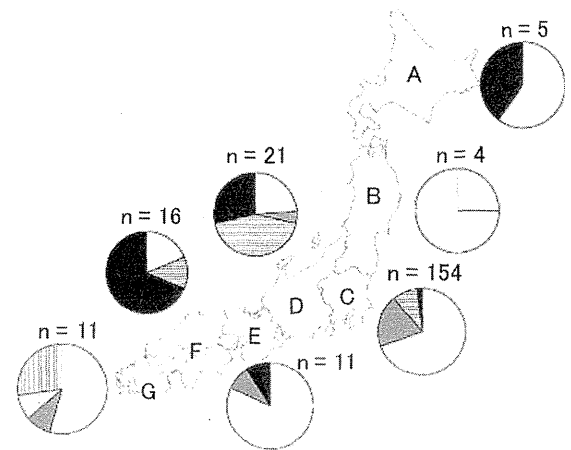


Fig. 1 - Distribution pattern of occurrence of chronic HP in Japan. The proportions of chronic HP in 7 areas are shown (A-G). White, bird-related HP; gray, summer-type HP; horizontal lines, home-related HP; dotted lines, farmer's lung; vertical lines, isocyanate-induced HP; black, others. The total number of cases is shown on the circle graphs.

Table 1 - Summary by type of chronic HP^a

Type	BRHP	SHP	HRHP	FL	IHP	Other	Total
Number	134	33	25	4	3	23	222
Gender (M/F)	62/72	20/13	16/9	4/0	3/0	15/8	120/102
Smoking history (never/ex/current)	67/44/16	14/16/3	9/13/2	1/3/0	0/0/3	10/13/0	101/89/24
Age of diagnosis (years)	64.0 [55.0-70.0] (134)	65.0 [60.0-72.0] (32)	69.0 [60.5-74.5] (25)	70.5 [65.5-77.6] (4)	52.0 [51.0-63.0] (3)	63.0 [57.0-69.0] (23)	64.0 [57.0-70.5] (221)
Onset to the first visit (months)	13.0 [2.0-43.0] (106)	11.0 [4.0-61.0] (27)	23.0 [4.0-55.0] (23)	34.0 [1.0-240.0] (3)	4.0 [2.0-7.0] (3)	32.0 [8.0-44.0] (21)	15.0 [3.0-44.0] (183)
Observation period (months)	38.0 [19.8-59.5] (105)	38.0 [17.0-55.0] (31)	31.0 [14.0-48.5] (25)	6.0 [6.0-6.0] (1)	24.0 [12.0-24.0] (3)	24.5 [7.5-31.0] (22)	31.0 [16.0-53.0] (187)

BRHP, bird-related hypersensitivity pneumonitis; SHP, summer-type hypersensitivity pneumonitis; HRHP, home-related hypersensitivity pneumonitis; FL, farmer's lung; IHP, isocyanate-induced hypersensitivity pneumonitis; Other, other types of chronic hypersensitivity pneumonitis.

^a Values are expressed as median [25th-75th percentile], with the estimated number of patients in parentheses.

Table 2 - Symptoms and physical findings^a

Type	BRHP	SHP	HRHP	FL	IHP	Other	Total
Fever	17/131 (13.0)	6/32 (18.8)	8/25 (32.0)	1/4 (25.0)	1/3 (66.7)	2/22 (9.1)	35/217 (16.1)
Cough	99/130 (76.2)	22/32 (68.8)	16/25 (64.0)	3/4 (75.0)	3/3 (100.0)	16/23 (69.6)	159/217 (73.3)
Sputum	39/130 (30.0)	14/32 (43.8)	5/24 (20.8)	1/4 (25.0)	2/3 (66.7)	5/22 (22.7)	66/215 (30.7)
Dyspnea	94/129 (72.9)	23/32 (71.9)	16/25 (64.0)	3/4 (75.0)	3/3 (100.0)	18/23 (78.3)	157/216 (72.7)
Fine crackles	103/111 (92.8)	23/27 (85.2)	20/22 (90.9)	2/3 (66.7)	3/3 (100.0)	20/21 (95.2)	171/187 (91.4)
Clubbed fingers	28/109 (25.7)	11/25 (44.0)	9/22 (40.9)	1/2 (50.0)	1/3 (33.3)	4/14 (28.6)	54/165 (32.7)

BRHP, bird-related hypersensitivity pneumonitis; SHP, summer-type hypersensitivity pneumonitis; HRHP, home-related hypersensitivity pneumonitis; FL, farmer's lung; IHP, isocyanate-induced hypersensitivity pneumonitis; Other, other types of chronic hypersensitivity pneumonitis.

^a The percentage of positive ratios is expressed in parentheses.

Table 3 - Laboratory findings^a

Type	BRHP	SHP	HRHP	FL	IHP	Other	Total
WBC (μ L)	6700 [5700-8000] (127)	7200 [6000-9100] (33)	6900 [5900-8250] (25)	6445 [4705-8155] (4)	5600 [4600-9500] (3)	6895 [6003-8700] (22)	6800 [5700-8200] (214)
CRP (mg/dL)	0.22 [0.10-0.75] (129)	0.20 [0.10-0.80] (33)	0.30 [0.10-0.90] (25)	1.10 [0.23-1.60] (3)	0.46 [0.11-0.52] (3)	0.12 [0.00-0.60] (22)	0.23 [0.10-0.80] (215)
LDH (IU/L)	242 [209-298] (129)	237 [230-255] (33)	228 [199-279] (25)	219 [208-373] (3)	299 [228-339] (3)	222 [202-272] (21)	238 [209-287] (214)
KL-6 (U/mL)	1670 [923-3187] (112)	1250 [759-2090] (27)	1134 [746-4896] (22)	2510 [1020-2990] (3)	5410 [3470-9000] (3)	1196 [667-1819] (20)	1448 [872-3170] (187)
SP-D (ng/mL)	228 [136-427] (86)	234 [180-431] (25)	264 [140-342] (20)	648 [340-955] (2)	929 [460-1180] (3)	250 [113-342] (9)	240 [141-437] (145)
Positive ratio							
ANA	13/69 (18.8%)	6/22 (27.3%)	7/24 (29.2%)	0/4 (0%)	0/3 (0.0%)	8/21 (38.1%)	34/140 (24.3%)
RF	21/80 (26.3%)	10/26 (38.5%)	3/21 (14.3%)	1/3 (33.3%)	0/3 (0.0%)	3/21 (14.3%)	38/160 (23.8%)
MPO-ANCA	3/55 (5.5%)	2/23 (8.7%)	0/21 (0.0%)	-	0/3 (0.0%)	0/15 (0.0%)	5/117 (4.3%)
PR3-ANCA	0/29 (0.0%)	0/11 (0.0%)	0/14 (0.0%)	-	0/3 (0.0%)	0/12 (0.0%)	0/69 (0.0%)

BRHP, bird-related hypersensitivity pneumonitis; SHP, summer-type hypersensitivity pneumonitis; HRHP, home-related hypersensitivity pneumonitis; FL, farmer's lung; IHP, isocyanate-induced hypersensitivity pneumonitis; Other, other types of chronic hypersensitivity pneumonitis; WBC, white blood cell count; CRP, C-reactive protein; LDH, lactate dehydrogenase; KL-6, Krebs von den Lungen 6; SP-D, surfactant protein D; ANA, anti-nuclear antibody; RF, rheumatoid factor; MPO-ANCA, myeloperoxidase anti-neutrophil cytoplasmic antibody; PR3-ANCA, proteinase-3 anti-neutrophil cytoplasmic antibody.

^a Values are expressed as median [25th-75th percentile], with the estimated number of patients in parentheses.

antibody, rheumatoid factor, and myeloperoxidase anti-neutrophil cytoplasmic antibody were positive in 24.3%, 23.8%, and 4.3% of the cases, respectively. None of the patients, however, manifested clinical features suggestive of collagen vascular disease.

3.4. Pulmonary function tests

Restrictive impairment and decreases in diffusing capacity were observed (Table 4). The median percentages of predicted vital capacity and forced vital capacity were 78.7% and 76.7%, respectively, and the median percentage of predicted carbon monoxide diffusing capacity was 55.9%. In contrast, the median percentage of forced expiratory volume in 1 s was within normal limits (83.8%).

3.5. BAL

Table 4 shows the profile of BAL fluid at the time of diagnosis of chronic HP. The median proportion of lymphocytes was high (24.5%), and the median CD4/CD8 ratio was 2.00. Although few in number, the patients with isocyanate-induced HP had the highest median percentage of lymphocytes and the lowest median CD4/CD8 ratio among the 6 HP groups. The CD4/CD8 ratio of those with isocyanate-induced HP was significantly lower than that of those with home-related HP.

3.6. Imaging

Radiographs and CT scans were evaluated on the basis of the characteristics of the shadows observed (Table 5). The typical radiography findings were ground-glass opacity (82.5%) and

Table 4 – Pulmonary function test and bronchoalveolar lavage fluid findings^a

Type	BRHP	SHP	HRHP	FL	IHP	Other	Total
Pulmonary function test							
%VC (%)	77.8 [62.7–94.1] (123)	82.4 [71.7–92.0] (33)	73.9 [65.5–88.6] (18)	96.3 [57.3–100.9] (4)	86.8 [86.8–86.8] (1)	78.8 [55.8–96.1] (20)	78.7 [64.5–92.9] (199)
%FVC (%)	73.5 [59.1–87.7] (71)	79.4 [65.2–90.6] (25)	75.1 [57.3–81.0] (16)	95.8 [56.1–101.5] (4)	86.2 [86.2–86.2] (1)	75.5 [58.4–87.7] (15)	76.7 [59.8–87.7] (132)
FEV _{1.0} (%)	82.9 [78.6–89.1] (120)	81.4 [78.4–86.0] (33)	86.3 [81.8–91.8] (22)	83.8 [71.9–103.0] (4)	75.9 [75.9–75.9] (1)	84.7 [82.7–88.3] (20)	83.8 [78.8–88.3] (200)
%DLco (%)	55.5 [44.2–78.7] (102)	60.5 [38.3–70.9] (27)	54.1 [47.3–73.9] (14)	71.2 [32.7–108.5] (4)	31.6 [31.6–31.6] (1)	54.2 [43.0–71.7] (17)	55.9 [44.0–75.0] (165)
Bronchoalveolar lavage fluid							
Macrophages (%)	66.0 [23.8–84.6] (114)	62.3 [20.4–84.5] (22)	71.1 [63.0–86.0] (23)	27.5 [19.5–55.0] (4)	14.8 [8.1–16.3] (3)	70.7 [42.4–83.6] (23)	66.2 [26.3–84.3] (189)
Lymphocytes (%)	25.0 [10.0–71.3] (117)	27.3 [10.4–74.3] (22)	17.0 [7.4–25.1] (23)	43.6 [18.0–56.2] (4)	84.3 [67.5–86.1] (3)	24.5 [5.5–48.8] (23)	24.5 [9.8–64.8] (192)
Neutrophils (%)	2.0 [0.6–4.7] (113)	2.6 [1.3–5.7] (22)	1.5 [0.6–7.9] (23)	4.5 [1.3–40.9] (4)	0.7 [0.4–0.7] (3)	2.0 [1.0–6.0] (23)	2.0 [0.7–5.3] (188)
Eosinophils (%)	1.0 [0.1–2.9] (113)	1.4 [0.7–3.0] (22)	0.8 [0.2–3.2] (23)	2.6 [0.3–12.7] (4)	5.3 [0.1–15.6] (3)	1.0 [0.6–3.0] (23)	1.2 [0.4–3.0] (188)
CD4/CD8 ratio	1.96 [0.12–3.56] (106)	1.53 [0.57–4.24] (17)	2.33 [†] [1.24–5.20] (21)	0.88 [0.26–1.91] (4)	0.09 [†] [0.03–0.11] (3)	2.80 [1.70–3.80] (23)	2.00 [1.00–3.75] (174)

BRHP, bird-related hypersensitivity pneumonitis; SHP, summer-type hypersensitivity pneumonitis; HRHP, home-related hypersensitivity pneumonitis; FL, farmer's lung; IHP, isocyanate-induced hypersensitivity pneumonitis; Other, other types of chronic hypersensitivity pneumonitis; %VC, vital capacity percentage predicted; %FVC, forced vital capacity percentage predicted; FEV_{1.0}%, ratio of forced expiratory volume for 1 s to forced vital capacity; %DLco, diffusing lung capacity for carbon monoxide percentage predicted.

^a Values are expressed as median [25th–75th percentile], with the estimated number of patients in parentheses.

[†] *p* < 0.01 using χ^2 test.

volume loss (43.1%). The major findings of CT scan of the chest were areas with ground-glass attenuation (85.7%) and interlobular septal thickening (60.8%), followed by honeycombing (41.0%). Laterality of these findings was noted in only 9.4% of the patients in whom the findings were observed. Distribution of abnormal chest shadows was identified predominantly in the lower lobes in 41.7% of the cases, in the whole lung in 44.9%, and in the upper lobes in 13.4%. The percentages of interlobular septal thickening and honeycombing in those with summer-type HP were higher than in those with bird-related HP.

3.7. Pathological findings

Ninety-three of the cases were evaluated using surgical lung biopsy specimens (Table 6). Centrilobular fibrosis (74.5%) and alveolitis (66.0%) were the primary findings. Fibroblastic foci, honeycombing, and perilobular fibrosis, all conditions frequently seen in IPF, were observed in 41.5%, 35.1%, and 34.0%

of the cases, respectively. Giant cells and granulomas were observed in 37.2% and 30.2% of the cases, respectively. Additionally, 20 cases could not be detected with causative antigens, even if they were diagnosed histologically. The percentages of centrilobular fibrosis, honeycombing, perilobular fibrosis, lymphoid follicles, bronchiolitis, and organizing pneumonia in those with home-related HP were significantly higher than in those with bird-related HP. Moreover, the percentage of perilobular fibrosis in those with summer-type HP was significantly higher than in those with bird-related HP.

3.8. Immunological findings

Table 7 shows the results of the immunological tests. Bird-related HP and home-related HP had high positive ratios of specific antibody. The positive ratios for the lymphocyte proliferation test, environment provocation test, and inhalation provocation test were 72.4%, 59.6%, and 80.0%, respectively.

Table 5 - Radiography and CT findings^a

Type	BRHP	SHP	HRHP	FL	IHP	Other	Total
X-ray							
Ground-glass opacity	85.1	85.2	69.6	0.0	66.7	85.7	82.5
Volume loss	38.1	58.3	52.6	100.0	0.0	47.6	43.1
Linear shadow	27.1	14.8	39.1	100.0	33.3	57.1	30.7
Infiltration	32.5	25.9	39.1	0.0	33.3	4.8	29.1
Micronodule	28.1	11.1	34.8	0.0	33.3	19.0	25.4
Laterality	8.2	13.6	20.0	0.0	0.0	20.0	9.9
Distribution upper/ lower/ whole	14.2/46.0/39.8	7.4/70.4/22.2	9.5/57.1/33.3	100.0/0.0/0.0	33.3/33.3/33.3	4.8/42.9/52.4	12.4/50.0/37.6
CT							
Ground-glass opacity	88.6	85.2	82.6	100.0	100.0	71.4	85.7
Interlobular septal thickening	54.4 [†]	85.2 [†]	65.2	0.0	33.3	66.7	60.8
Honeycombing	33.1 [†]	63.6 [†]	52.0	100.0	0.0	43.5	41.0
Interlobular reticular shadow	36.0	40.7	52.2	0.0	0.0	61.9	40.7
Micronodule	39.5	40.7	26.1	0.0	33.3	33.3	37.0
Consolidation	33.3	29.6	34.8	0.0	33.3	14.3	30.7
Laterality	6.4	20.0	18.2	0.0	0.0	5.3	9.4
Distribution upper/ lower/ whole	16.7/34.2/49.1	7.7/65.4/26.9	9.1/54.5/36.4	0.0/100.0/0.0	33.3/33.3/33.3	4.8/38.1/57.1	13.4/41.7/44.9

BRHP, bird-related hypersensitivity pneumonitis; SHP, summer-type hypersensitivity pneumonitis; HRHP, home-related hypersensitivity pneumonitis; FL, farmer's lung; IHP, isocyanate-induced hypersensitivity pneumonitis; Other, other types of chronic hypersensitivity pneumonitis.

^a Values are expressed as the percentage of positive ratio.

* $p < 0.01$ using χ^2 test.

Table 6 - Pathological findings^a

Type	BRHP (n=56)	SHP (n=5)	HRHP (n=14)	Other (n=18)	Total (N=93)
Centrilobular fibrosis	73.2 [†]	100.0	100.0 [†]	55.6	74.5
Alveolitis	64.3	100.0	85.7	44.4	66.0
Fibroblastic foci	30.4	60.0	57.1	61.1	41.5
Giant cells	30.4	40.0	57.1	44.4	37.2
Honeycombing	23.2 [§]	20.0	64.3 [§]	55.6	35.1
Perilobular fibrosis	21.4 [‡]	100.0 [‡]	71.4 [‡]	27.8	34.0
Granulomas	28.1	40.0	26.7	38.9	30.2
Lymphoid follicles	12.5 [§]	40.0	64.3 [§]	33.3	25.5
Bronchiolitis	14.3 [§]	20.0	64.3 [§]	11.1	21.3
Organizing pneumonia	7.1 [‡]	20.0	42.9 [‡]	11.1	13.8

BRHP, bird-related hypersensitivity pneumonitis; SHP, summer-type hypersensitivity pneumonitis; HRHP, home-related hypersensitivity pneumonitis; Other, other types of chronic hypersensitivity pneumonitis.

^a Values are expressed as the percentage of positive ratio.

[†] $p < 0.05$ using χ^2 test.

[‡] $p < 0.01$ using χ^2 test.

[§] $p < 0.001$ using χ^2 test.

3.9. Treatment and prognosis

Steroids were administered to 134 patients (69.1%) and were effective in 79.2% of the patients who received them. There were no differences in the efficacy of steroids among the 6 groups. Immunosuppressants were administered to 42 patients as combination therapy with steroids and were effective in 39.4% of the patients who received them. The median survival time was 83 months, and no difference in survival curve was found among the 3 major subgroups (Fig. 2).

4. Discussion

The most prevalent variant of chronic HP in the present survey was bird-related HP, accounting for 60.3% of cases of chronic HP. Although there were some differences regarding CT and pathological findings between bird-related HP and other subtypes, the other clinical features, including symptoms, physical findings, laboratory data, pulmonary function tests, BAL, and prognosis, were similar among them. Several

Table 7 - Immunological findings^a

Type	BRHP	SHP	HRHP	FL	IHP	Other	Total
Specific antibody	97/118 (82.2)	31/33 (93.9)	2/21 (9.5)	-	3/3 (100.0)	4/7 (57.1)	137/182 (75.3)
Lymphocyte proliferation test	59/82 (72.0)	2/2 (100.)	2/2 (100.0)	1/1 (100.0)	-	-	63/87 (72.4)
Environment provocation test	15/24 (62.0.5)	9/14 (64.3)	8/17 (47.1)	-	-	2/2 (100.0)	34/57 (59.6)
Inhalation provocation test	42/51 (82.4)	0/1 (0.0)	0/1 (0.0)	-	-	2/2 (100.0)	44/55 (80.0)

BRHP, bird-related hypersensitivity pneumonitis; SHP, summer-type hypersensitivity pneumonitis; HRHP, home-related hypersensitivity pneumonitis; FL, farmer's lung; IHP, isocyanate-induced hypersensitivity pneumonitis; Other, other types of chronic hypersensitivity pneumonitis.

^a The percentage of positive ratio is expressed in parentheses.

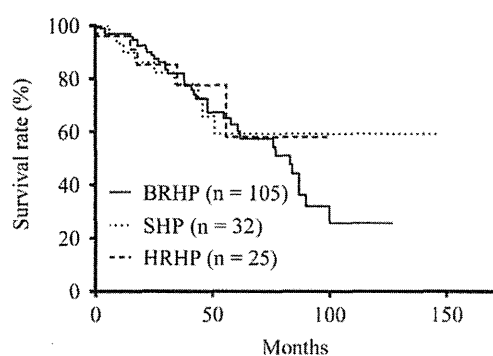


Fig. 2 - Survival curve of the 3 major groups with chronic HP. The survival of those with bird-related HP (BRHP), summer-type HP (SHP), and home-related HP (HRHP) is shown using a Kaplan-Meier curve. There is no significant difference among the groups by log-rank test.

reasons may account for this finding. First, clinicians have grown more familiar with bird-related HP over the past decade, and more clinicians are mindful of the antigen responsible for pulmonary fibrosis [9-12]. Second, the public has ample chance of exposure to avian antigens through contact with living birds, poultry manure, duvets and jackets made of bird feathers, and the like [8,13-15]. Third, the immune response to avian proteins may differ from that to other antigens, and the turnover of avian proteins in the lungs may be decreased [16,17]. Finally, more immunological methods are available for the diagnosis of bird-related HP compared with other HPs.

Geographical, social, and occupational factors determine the particular types of HP found throughout the world. Lacasse et al. demonstrated that BFL was the most common subtype among all chronic forms of HP (80.9%) [1]. In a report from the Mayo Clinic on 85 cases with HP of all types, 66 (78%) had chronic HP, and the common causative antigens were avian antigens (34%) and *Mycobacterium avium* complex in hot tub water (21%) (only a few cases with hot tub lung have been reported in Japan) [9]. Farmer's lung accounted for 11% of cases, and another 9% were related to household mold exposure. Selman et al. reported that the most common

subgroup of HP diagnosed in Mexico was BFL [18]. The most common subgroup of chronic HP in small studies from Turkey and China was also BFL [10,19]. These lines of evidence suggest that the major diagnosis of chronic HP may be a bird-related HP in different areas of the world.

Some studies have reported that patients with bird-related HP are predominantly female [9,11]. By way of explanation, Selman et al. proposed that the proportion of HP cases caused by domestic exposure to avian antigens may be higher in women than in men. In our study, many of the patients with bird-related HP were men. In cases not directly exposed to birds, we identified the causative agents as poultry manure and duvets and jackets stuffed with bird feathers.

KL-6 and SP-D, which are established markers of pulmonary fibrosis, were both elevated, whereas C-reactive protein level and white blood cell count, which are markers of inflammation, were normal. As in the case with IPF, the main pathogenesis of chronic HP is thought to be irreversible pulmonary fibrosis and not an inflammatory process. We found a significant correlation between KL-6 and SP-D in our population ($r=0.497$, $p<0.0001$).

BAL fluid in patients with chronic HP revealed relative lymphocytosis, but this BAL finding is not specific for a diagnosis of chronic HP. Previous studies have shown that the CD4/CD8 ratio in BAL fluid may vary significantly according to the clinical presentation of the disease, the biological characteristics of the inhalation antigen, the exposure to the causative antigen at the time of diagnosis, the immune susceptibility of particular patients, and a history of smoking [20]. An insidious onset of chronic HP was associated with lung fibrosis and relatively elevated CD4+ T cells in BAL fluid [21,22]. The CD4/CD8 ratio in this survey was 2.00 and the median CD4/CD8 ratio of isocyanate-induced HP was the lowest, which is similar to that reported in the previous survey [4].

CT is an essential tool in the diagnostic evaluation of interstitial lung diseases. The CT features of chronic HP frequently overlap those of nonspecific interstitial pneumonia and unusual interstitial pneumonia. Honeycombing and lower zone predominance of abnormalities, 2 hallmark features of IPF, were seen in 41.0% and 41.7% of the patients in the present survey, respectively. As in previous reports [11,12,23-25], CT of patients with chronic HP revealed high frequencies of ground-glass opacity and centrilobular nodules. The CT features that best

differentiated chronic HP from IPF and nonspecific interstitial pneumonia are reported to include lobular areas with decreased attenuation and vascularity, centrilobular nodules, and no lower zone predominance of abnormalities [24], yet almost half of the patients in our survey had lower zone predominance of abnormalities.

Lung biopsy plays an important role in identifying patients for whom no offending antigen is discovered, particularly those with persistent symptoms. We expanded an understanding of the pathology of chronic HP, and the number of cases diagnosed by surgical lung biopsies seems to have increased recently. The pathological features of chronic HP typically comprise an overlapping unusual interstitial pneumonia-like pattern, a nonspecific interstitial pneumonia-like pattern, and centrilobular fibrosis. In chronic HP, fibrosis is represented by irregular linear opacities, traction bronchiectasis, lobar volume loss, and honeycombing [26]. Chronic HP is more challenging to diagnose than acute HP, because granulomas can rarely be found. Granulomas were detected in only 5 of 26 cases of chronic HP (19.2%) reported by Ohtani et al. [6]. Granulomas were observed in 30.2% of cases in this larger study, but we believe them to be useful for differentiating chronic HP from IPF, because they are usually absent in the latter disease. Although we have no clear explanation about the differences between bird-related HP, summer-type HP, and home-related HP on CT and pathological findings, we supposed that different inhalation antigens might comprise different phenotypes.

Our evaluations of immunological findings included antibodies to the causative antigens, the lymphocyte proliferation test, the inhalation provocation test, and the environment provocation test. The positive ratios were high in all of the immunological tests performed. Positive serologic test results confirm prior exposure and sensitization to an antigen but do not suffice in making the diagnosis of HP in the absence of an appropriate clinical and radiologic context. Furthermore, the absence of precipitating antibodies does not exclude the diagnosis of HP. Serum precipitins, however, may be useful to identify the causative agent once the diagnosis has been established. Only a limited number of institutions are equipped to perform immunological examinations, especially the lymphocyte proliferation test and inhalation provocation test. A previous study by Ramírez-Venegas et al. also demonstrated the diagnostic utility of a provocation test with pigeon serum in patients with subacute/chronic pigeon breeder's disease [13].

Antigen avoidance is the key element in the treatment of patients with HP. Complete cessation of exposure to the provoking antigen is the appropriate management, yet some of the patients surveyed showed a gradual deterioration even after antigen avoidance. Steroids were administered to 134 patients (69.1%) and were effective in 79.2% of the patients who received them. In the earlier epidemiological survey [4], the efficacy of steroid administration was limited in chronic HP but high in acute HP. We should also evaluate the effectiveness of pirfenidone and N-acetylcysteine, agents that have demonstrably prevented the decline of pulmonary function in recent studies [27,28].

Our survey has several limitations. Detailed clinical data were often difficult to collect retrospectively, and some values were missing. A workshop by the National Heart, Lung, and Blood Institute proposed the classifications of "recurrent" and

"insidious" for cases of chronic HP [29]. Although differences in clinical characteristics between the recurrent type and insidious type have been shown [21], we did not distinguish them in this survey. The numbers of cases with particular exposures (isocyanate-induced HP and farmer's lung) were too small to be statistically meaningful in detecting differences. This study may be partly influenced by a selection bias of hospitals we surveyed.

In conclusion, we collected data on 222 cases with chronic HP throughout Japan over the past decade. The proportion of bird-related HP was higher than in the previous epidemiological survey, and the proportions of isocyanate-induced HP and farmer's lung were lower. We should be mindful of causative antigens when diagnosing interstitial lung diseases.

Conflict of interest

This study was partly supported by a grant to the Diffuse Lung Diseases Research Group from the Ministry of Health, Labor and Welfare, Japan.

Nobuoki Kohno has received royalties as a discoverer of KL-6.

Tsukasa Okamoto, Yasunari Miyazaki, Takashi Ogura, Kingo Chida, Shigeru Kohno, Hiroyuki Taniguchi, Shinobu Akagawa, Yoshiro Mochizuki, Kohei Yamauchi, Hiroki Takahashi, Takeshi Johkoh, Sakae Homma, Kazuma Kishi, Soichiro Ikushima, Satoshi Konno, Michiaki Mishima, Ken Ohta, Yasuhiko Nishioka, Nobuyuki Yoshimura, Mitsuru Munakata, Kentaro Watanabe, Yoshihiro Miyashita, and Naohiko Inase have no potential conflicts of interest.

Acknowledgments

The authors thank Makito Yasui and Koji Unoura, Tokyo Medical and Dental University, for arranging the questionnaire and their assistance in conducting this survey.

REFERENCES

- [1] Lacasse Y, Selman M, Costabel U, et al. Classification of hypersensitivity pneumonitis: a hypothesis. *Int Arch Allergy Immunol* 2009;149:161-6.
- [2] Agostini C, Trentin L, Facco M, et al. New aspects of hypersensitivity pneumonitis. *Curr Opin Pulm Med* 2004;10:378-82.
- [3] Pérez-Padilla R, Salas J, Chapela R, et al. Mortality in Mexican patients with chronic pigeon breeder's lung compared with those with usual interstitial pneumonia. *Am Rev Respir Dis* 1993;148:49-53.
- [4] Yoshizawa Y, Ohtani Y, Hayakawa H, et al. Chronic hypersensitivity pneumonitis in Japan: a nationwide epidemiologic survey. *J Allergy Clin Immunol* 1999;103:315-20.
- [5] Ando M, Konishi K, Yoneda R, et al. Difference in the phenotypes of bronchoalveolar lavage lymphocytes in patients with summer-type hypersensitivity pneumonitis, farmer's lung, ventilation pneumonitis, and bird fancier's lung: report of a nationwide epidemiologic study in Japan. *J Allergy Clin Immunol* 1991;87:1002-9.
- [6] Ohtani Y, Saiki S, Kitaichi M, et al. Chronic bird fancier's lung: histopathological and clinical correlation. An application of

- the 2002 ATS/ERS consensus classification of the idiopathic interstitial pneumonias. *Thorax* 2005;60:665-71.
- [7] Yoshizawa Y, Miyake S, Sumi Y, et al. A follow-up study of pulmonary function tests, bronchoalveolar lavage cells, and humoral and cellular immunity in bird fancier's lung. *J Allergy Clin Immunol* 1995;96:122-9.
- [8] Ohtani Y, Kojima K, Sumi Y, et al. Inhalation provocation tests in chronic bird fancier's lung. *Chest* 2000;118:1382-9.
- [9] Hanak V, Golbin JM, Ryu JH. Causes and presenting features in 85 consecutive patients with hypersensitivity pneumonitis. *Mayo Clin Proc* 2007;82:812-6.
- [10] Cımrın AH, Göksele O, Demirel YS. General aspects of hypersensitivity pneumonitis in Turkey. *Tuberk Toraks* 2010;58:242-51.
- [11] Morell F, Roger A, Reyes L, et al. Bird fancier's lung: a series of 86 patients. *Medicine (Baltimore)* 2008;87:110-30.
- [12] Lima M, Coletta E, Ferreira R, et al. Subacute and chronic hypersensitivity pneumonitis: histopathological patterns and survival. *Respir Med* 2009;103:508-15.
- [13] Ramírez-Venegas A, Sansores RH, Pérez-Padilla R, et al. Utility of a provocation test for diagnosis of chronic pigeon Breeder's disease. *Am J Respir Crit Care Med* 1998;158:862-9.
- [14] Inase N, Ohtani Y, Sumi Y, et al. A clinical study of hypersensitivity pneumonitis presumably caused by feather duvets. *Ann Allergy Asthma Immunol* 2006;96:98-104.
- [15] Koschel D, Wittstruck H, Renck T, et al. Presenting features of feather duvet lung. *Int Arch Allergy Immunol* 2010;152:264-70.
- [16] Edwards JH, Barboriak JJ, Fink JN. Antigens in pigeon breeders' disease. *Immunology* 1970;19:729-34.
- [17] McSharry C, Anderson K, Boyd G. A review of antigen diversity causing lung disease among pigeon breeders. *Clin Exp Allergy* 2000;30:1221-9.
- [18] Selman M, Lacasse Y, Pardo A, et al. Hypersensitivity pneumonitis caused by fungi. *Proc Am Thorac Soc* 2010;7:229-36.
- [19] Wang P, Xu ZJ, Xu WB, et al. Clinical features and prognosis in 21 patients with extrinsic allergic alveolitis. *Chin Med Sci J* 2009;24:202-7.
- [20] Thomas M, von Eiff M, Brandt B, et al. Immunophenotyping of lymphocytes in bronchoalveolar lavage fluid. A new flow cytometric method vs standard immunoperoxidase technique. *Chest* 1995;108:464-9.
- [21] Ohtani Y, Saiki S, Sumi Y, et al. Clinical features of recurrent and insidious chronic bird fancier's lung. *Ann Allergy Asthma Immunol* 2003;90:604-10.
- [22] Murayama J, Yoshizawa Y, Ohtsuka M, et al. Lung fibrosis in hypersensitivity pneumonitis. Association with CD4+ but not CD8+ cell dominant alveolitis and insidious onset. *Chest* 1993;104:38-43.
- [23] Remy-Jardin M, Remy J, Wallaert B, et al. Subacute and chronic bird breeder hypersensitivity pneumonitis: sequential evaluation with CT and correlation with lung function tests and bronchoalveolar lavage. *Radiology* 1993;189:111-8.
- [24] Silva CI, Müller NL, Lynch DA, et al. Chronic hypersensitivity pneumonitis: differentiation from idiopathic pulmonary fibrosis and nonspecific interstitial pneumonia by using thin-section CT. *Radiology* 2008;246:288-97.
- [25] Buschman DL, Gamsu G, Waldron JA, et al. Chronic hypersensitivity pneumonitis: use of CT in diagnosis. *AJR Am J Roentgenol* 1992;159:957-60.
- [26] Patel RA, Sellami D, Gotway MB, et al. Hypersensitivity pneumonitis: patterns on high-resolution CT. *J Comput Assist Tomogr* 2000;24:965-70.
- [27] Taniguchi H, Ebina M, Kondoh Y, et al. Pirfenidone in idiopathic pulmonary fibrosis. *Eur Respir J* 2010;35:821-9.
- [28] Demedts M, Behr J, Buhl R, et al. High-dose acetylcysteine in idiopathic pulmonary fibrosis. *N Engl J Med* 2005;353:2229-42.
- [29] Fink JN, Ortega HG, Reynolds HY, et al. Needs and opportunities for research in hypersensitivity pneumonitis. *Am J Respir Crit Care Med* 2005;171:792-8.

Flagellin/TLR5 signaling potentiates airway serous secretion from swine tracheal submucosal glands

Soshi Muramatsu,¹ Tsutomu Tamada,¹ Masayuki Nara,² Koji Murakami,¹ Toshiaki Kikuchi,¹ Masahiko Kanehira,¹ Yoshio Maruyama,³ Masahito Ebina,¹ Toshihiro Nukiwa,⁴ and Masakazu Ichinose¹

Departments of ¹Respiratory Medicine, ²Comprehensive Medicine, and ³Physiology I, Tohoku University Graduate School of Medicine, Sendai; ⁴South Miyagi Medical Center, Miyagi, Japan

Submitted 21 February 2013; accepted in final form 4 October 2013

Muramatsu S, Tamada T, Nara M, Murakami K, Kikuchi T, Kanehira M, Maruyama Y, Ebina M, Nukiwa T, Ichinose M. Flagellin/TLR5 signaling potentiates airway serous secretion from swine tracheal submucosal glands. *Am J Physiol Lung Cell Mol Physiol* 305: L819–L830, 2013. First published October 4, 2013; doi:10.1152/ajplung.00053.2013.—Airway serous secretion is essential for the maintenance of mucociliary transport in airway mucosa, which is responsible for the upregulation of mucosal immunity. Although there are many articles concerning the importance of Toll-like receptors (TLRs) in airway immune systems, the direct relationship between TLRs and airway serous secretion has not been well investigated. Here, we focused on whether TLR5 ligand flagellin, which is one of the components of *Pseudomonas aeruginosa*, is involved in the upregulation of airway serous secretion. Freshly isolated swine tracheal submucosal gland cells were prepared, and the standard patch-clamp technique was applied for measurements of the whole cell ionic responses of these cells. Flagellin showed potentiating effects on these oscillatory currents induced by physiologically relevant low doses of acetylcholine (ACh) in a dose-dependent manner. These potentiating effects were TLR5 dependent but TLR4 independent. Both nitric oxide (NO) synthase inhibitors and cGMP-dependent protein kinase (cGK) inhibitors abolished these flagellin-induced potentiating effects. Furthermore, TLR5 was abundantly expressed on tracheal submucosal glands. Flagellin/TLR5 signaling further accelerated the intracellular NO synthesis induced by ACh. These findings suggest that TLR5 takes part in the airway mucosal defense systems as a unique endogenous potentiator of airway serous secretions and that NO/cGMP/cGK signaling is involved in this rapid potentiation by TLR5 signaling.

Ca²⁺-activated Cl⁻ channel; nitric oxide; cGMP-dependent protein kinase; patch-clamp; *Pseudomonas aeruginosa*

TRACHEAL SUBMUCOSAL GLANDS secrete mucin, various enzyme proteins, and electrolytes (therefore, water), which serve as a nonspecific airway defense mechanism. Additionally, submucosal glands secrete immunoglobulins to neutralize many microbes, serving as a specific airway defense mechanism (34). Among these airway mucosal defense systems, airway serous secretion plays important roles in hydrating airway surfaces and flushing mucin glycoproteins out of the ducts, contributing to the maintenance of mucociliary transport (2, 4, 10, 24, 48). Human, feline, and swine tracheal gland acinar cells generate ionic currents in response to relatively low doses of cholinergic and α -adrenergic stimuli, and these currents are activated by

the intracellular Ca²⁺ concentration ([Ca²⁺]_i) raised by these neurotransmitters (16, 31, 38, 44, 45). The Ca²⁺-activated Cl⁻ channel (CaCC) may play an important role in physiological basal secretions in the airways. It has recently become known that CaCC composes a newly identified transmembrane protein with unknown function, 16, Ano 1 (TMEM16A), which exists in both the airway surface epithelium and submucosal glands (28, 33). Concerning the electrophysiological characteristics of CaCC, we have reported that tyrosine kinase, cyclic-ADP ribose, and nitric oxide (NO)/cGMP/cGMP-dependent protein kinase (cGK) are involved in the intracellular pathway of oscillatory ionic currents evoked by low doses of acetylcholine (ACh) (18, 39, 44).

Toll-like receptors (TLRs) are known to be key proteins that recognize distinct pathogen-associated molecular patterns (PAMPs) and activate innate immune responses as well as antigen-specific adaptive immunity (1, 22). It is also known that airway epithelial cells express several kinds of TLRs and that the activation of TLRs on epithelial cells induces the production of several cytokines, chemokines, and antimicrobial peptides (11, 12, 40). In chronic inflammatory airway diseases like chronic obstructive pulmonary disease (COPD), *Pseudomonas aeruginosa* (*P. aeruginosa*) often colonizes the airway mucosal surface and sometimes causes repeated respiratory infections, resulting in exacerbations of these diseases (42). *P. aeruginosa* involves LPS in its cell wall and flagellin in its flagellum, each of which are known to be a ligand for TLR4 and TLR5, respectively. We have recently shown that the TLR4 ligand functions as a unique, endogenous potentiator of serous secretion from tracheal gland acinar cells (31). However, because LPS is known to be a prototypical example of endotoxin, it may cause nonspecific effects other than as a TLR4 ligand *in vivo*. On the other hand, although it has become increasingly clear that flagellin/TLR5 signaling plays an important role in the airway mucosal innate immunity systems (35), it is not well known whether flagellin potentiates airway serous secretion.

Here, we investigated the potential role of flagellin in serous secretion from tracheal submucosal glands. Flagellin potentiated the electrolyte secretion from tracheal gland acinar cells, and its potentiating effect was reproduced only when cells were stimulated by physiologically relevant low doses of ACh. The intracellular mechanism of this rapid action appeared to be induced by both NO and cGK. These potentiating effects induced by flagellin were TLR5 dependent but TLR4 independent. Flagellin caused a significant potentiation in ACh-induced intracellular NO synthesis, which was almost abolished by treatment with anti-TLR5 blocking antibody. These findings suggest that TLR5 is also involved in the airway mucosal

Address for reprint requests and other correspondence: T. Tamada, Dept. of Respiratory Medicine, Tohoku Univ. Graduate School of Medicine, 1-1 Seiryomachi, Aoba-ku, Sendai 980-8574, JAPAN (e-mail: tamada@rm.med.tohoku.ac.jp).

defense systems as a unique endogenous potentiator of electrolyte-water secretion from submucosal gland acinar cells and that NO/cGMP/cGK signaling is involved in this rapid TLR5 signaling pathway.

MATERIALS AND METHODS

Preparation of cells. Swine tracheas were obtained at a local slaughterhouse immediately after the animals had been killed and were transported to our laboratory in an ice-cold extracellular solution. The external surfaces of tracheas were cleaned of fat and connective tissues and cut into rings 3–4 cm long. The posterior (membranous) strip of tracheal walls were then excised longitudinally, leaving attached to both sides a cartilaginous portion of about 1 cm in width, and were fixed by pins in the extracellular solution with the external wall side up. The outermost layer and thick smooth muscle layer were carefully removed. The submucosal glands could then be easily distinguished from the surrounding connective tissue under a stereoscopic microscope with the light shed horizontally. Fresh, unstained submucosal glands were isolated using two pairs of tweezers and microscissors. The isolated glands were further dispersed enzymatically by incubating them with enzyme solution containing collagenase (200 U/ml) and DL-DTT (0.31 mg/ml) for 30 min at 37°C. After dispersion and a wash with centrifugation at 180 g, the cells were resuspended in a standard extracellular solution until use, as reported previously (16, 17, 31, 38, 39, 44, 45). In a series of experiments investigating the effect of blocking antibodies, anti-TLR5 polyclonal antibody (10 µg/ml) or nonspecific IgG (10 µg/ml) was also preincubated with cells for 1 h at 37°C before use.

Electrical recordings. Ionic currents were measured with a patch-clamp amplifier (EPC9; HEKA Electronic, Lambrecht, Germany), low-pass filtered at 2.9 kHz, and monitored on both a built-in software oscilloscope and a thermal pen recorder (RECTI-HORIZ-8K; Nippondenki Sanei, Tokyo, Japan). Patch pipettes were made of borosilicate glass capillary with an outer diameter of 1.5 mm using a vertical puller (PP-83; Narishige Scientific Instruments, Tokyo, Japan) and had a tip resistance of 4–6 MΩ. The junction potential between the patch pipette and bath solution was nulled by an amplifier circuitry. After the establishment of a high-resistance (1 GΩ), tight seal, the whole cell configuration was obtained by rupturing the patch membrane with negative pressure applied to the pipette tip. Membrane currents were monitored at two different holding potentials (Hps), i.e., 0 and –80 mV, which roughly corresponded to the Cl[–] and K⁺ equilibrium potential. The double current monitoring, i.e., alternate recording of the ionic currents corresponding to Hp of 0 and –80 mV, was accomplished by applying 200-ms voltage pulses of –80 mV at a frequency of 2 Hz to the pipette voltage of 0 mV (16, 17, 31, 38, 39, 44, 45). The upward or downward deflection of the current tracing represents outward current (*I*_o) or inward current (*I*_i), respectively. Using proper channel inhibitors and ion substitution experiments, we have confirmed that the ACh-evoked *I*_o and *I*_i were carried mainly by K⁺ and Cl[–], both of which were dependent on intracellular Ca²⁺ concentration ([Ca²⁺]_i) (16, 17, 31, 38, 39, 44, 45). The solutions included an extracellular (bath) solution of 120 mM NaCl, 4.7 mM KCl, 1.13 mM MgCl₂, 1.2 mM CaCl₂, 10 mM glucose, and 10 mM HEPES and an intracellular (pipette) solution of 120 mM KCl, 1.13 mM MgCl₂, 0.5 mM EGTA, 1 mM Na₂ATP, 10 mM glucose, and 10 mM HEPES. The fluids were superfused over the cells by hydrostatic pressure-driven application (20–30 cmH₂O) through polyethylene tubes. All solutions were at pH 7.2, and all experiments were carried out at room temperature (22–25°C).

Quantification procedure. The procedure to estimate the ionic responses was also applied in our previous reports (17, 31, 44, 45). We first measured the area circumscribed with the current trace (*I*_o or *I*_i) and baseline for 20 s (area under curve₂₀) by using a digital planimeter (PLACOM, KP-92N; Koizumi, Tokyo, Japan). This area shows the net electric charge movements of 20-s duration in each

condition. The mean magnitudes of ionic currents for 20 s were next expressed by the following calculation: $I_{\text{mean}} = \text{area under curve}_{20}/20$ (pQ/s).

The effect of flagellin on the ACh-stimulated response was estimated by comparing data just before and after treatment with flagellin and was expressed as a percentage of pretreatment control values: $\%I_{\text{mean}}(\text{ACh} + \text{flagellin}) = [I_{\text{mean}}(\text{ACh} + \text{flagellin})/I_{\text{mean}}(\text{ACh})] \times 100$. The effect of cGK inhibitor on the responses induced by both ACh and flagellin was expressed as a percentage of $I_{\text{mean}}(\text{ACh} + \text{cGK inhibitor})$. $\%I_{\text{mean}}(\text{ACh} + \text{flagellin} + \text{cGK inhibitor}) = [I_{\text{mean}}(\text{ACh} + \text{flagellin} + \text{cGK inhibitor})/I_{\text{mean}}(\text{ACh} + \text{cGK inhibitor})] \times 100$. In some experiments, cGK inhibitor was replaced by NO synthase (NOS) inhibitors.

Immunofluorescent staining. After the swine were killed, fresh trachea or spleen blocks were prepared and cut into sections that were 3 mm × 10 mm. Tissue blocks were fixed by 10% buffered formalin and embedded in paraffin wax. The slides were heated in an autoclave at 121°C for 15 min in 0.1% sodium azide solution (pH 9.0; Nichirei, Tokyo, Japan) after deparaffinization for antigen retrieval. The sections (2.5-µm thickness) were incubated for 10 min with Protein Block Serum-Free (Dako, Carpinteria, CA) at room temperature to block nonspecific binding sites. After removal of the blocking solution, these sections were incubated with a rabbit polyclonal anti-TLR5 Ab specific to a 300–350-amino-acid residue (IMG-580, diluted 1:100; IMGEX, San Diego, CA) overnight at 4°C, as described previously (31). Antibody localization was performed using the DAKO EnVision/AP (Dako, Glostrup, Denmark) in darkness at room temperature for 50 min. Negative control samples were incubated with the secondary antibody only. The reaction was then completed with a substrate system using Permanent Red (Dako) as the chromogen. Sections were mounted in Slow Fade Antifade kit (Invitrogen, Carlsbad, CA) with DAPI (9).

Western blotting. Swine tracheal submucosal glands were lysed in RIPA buffer containing protease inhibitor cocktail and phosphatase inhibitor cocktail (Sigma-Aldrich, St. Louis, MO) and centrifuged at 15,000 g for 30 min at 4°C. Proteins were separated by SDS-PAGE (Novex 12% Tris-glycine) and transferred onto PVDF using iBlot (Invitrogen). Membranes were then blocked with PVDF Blocking Reagent for Can Get Signal (Toyobo, Osaka, Japan), immunoblotted with a rabbit polyclonal anti-TLR5 Ab (IMG-580, IMGEX) diluted with Can Get Signal Immunoreaction Enhancer Solution 1 (Toyobo) for 1 h at room temperature followed by the relevant horseradish peroxidase-conjugated secondary antibodies (Santa Cruz Biotechnology, Santa Cruz, CA) diluted with Can Get Signal Immunoreaction Enhancer Solution 2 (Toyobo) for 1 h at room temperature. The signals were visualized using the ECL detection system (GE Healthcare, Piscataway, NJ).

RT-PCR. Total RNA was isolated from swine tracheal submucosal gland cells and from swine spleen tissue as a positive control with an RNeasy Mini kit (QIAGEN, Tokyo, Japan). All cDNA was prepared by reverse transcription from 1 µg of total RNA, using oligo(dT)₂₀ primer and Superscript III reverse transcription (Invitrogen). The oligonucleotide primers used in PCR were as follows: swine TLR5 sense, 5'-TTT CTG GCA ATG GCT GGA CA-3'; antisense, 5'-TGG AGG TTG TCA AGT CCA TG-3'; swine β-actin sense, 5'-CAT CAC CAT CGG CAA CGA-3'; antisense, 5'-GCG TAG AGG TCC TTC CTG ATG T-3'. The PCR cycling conditions were 3 min at 94°C, followed by 35 cycles of 30 s at 94°C, 30 s at 60°C, and 30 s at 72°C. DNA fragments were analyzed in a 2% agarose gel electrophoresis.

Intracellular NO imaging with diaminofluorescein-2 diacetate. A highly specific fluorescent NO indicator, 4,5-diaminofluorescein (DAF-2), is known to be useful to estimate the amount of NO produced in the cytosol (25). The diacetate salt DAF-2DA is membrane permeable and is soon hydrolyzed at the ester bonds by the intracellular esterase, resulting in the membrane impermeable and relatively nonfluorescent compound, DAF-2. In the presence of oxy-

gen, NO combines with DAF-2 and forms the highly fluorescent triazolofluorescein DAF-2T. Peak excitation and emission wavelengths for DAF-2T occur at 495 and 515 nm, respectively. The fluorescence intensity shows a linear correlation with the concentration of DAF-2T, which is in parallel with the cellular production of NO. We have reported that freshly isolated swine tracheal glands showed good fluorescent responses with 10 μ M DAF-2DA (31, 44). All experiments were carried out under the same conditions. To prevent the fluorescence signaling from becoming attenuated, the fluorescence intensity was measured for 5 s every 5 min. The solutions were the same compositions as used in the patch-clamp experiments (see *Electrical recordings*) and were gassed with 100% O₂ during the measurements. The green levels in the areas of gland cells in the captured microfluorographs were determined by digital image software (NIS-Elements Basic Research version 3.00; Nikon, Tokyo, Japan). Thus we detected the increase in the amount of intracellular NO per unit area of gland acini at each measurement time. NO production was estimated as fold increases over the basal fluorescence intensity. The fluorescence intensities in Fig. 6 parallel the total amount of NO in the cytosol, not the newly synthesized NO per unit time. In Fig. 6, cells were preincubated with DAF-2DA for at least 40 min before each experiment.

Intracellular calcium assays. Freshly isolated swine tracheal submucosal gland cells were prepared as described in *Preparation of cells*. Cells were loaded with the ratiometric calcium indicator Fura-2 AM (Dojindo, Kumamoto, Japan) for 1 h and washed three times at room temperature, according to the manufacturer's protocol. They were plated with 190 μ l standard extracellular solutions in black-walled, clear-bottom Poly-D-Lysine-coated 96-well microplates (BD Biosciences, San Jose, CA) for 30 min at room temperature before measurements. The fluorescence reading (excitation at 340 and 380 nm and emission at 510 nm) was carried out in Flexstation 3 microplate reader (Molecular Devices, Sunnyvale, CA), every 4 s for 10 min. After control fluorescence intensities were measured for 120 s under unstimulated conditions, 20 μ l of ACh (30 nM final concentration) was automatically injected. Then, 22 μ l of either ACh (200 nM final concentration) or flagellin (1.0 μ g/ml final concentration) was injected at 240 s. Softmax Pro (Molecular Devices) was used for data analysis.

Statistics. Data were expressed as means \pm SE; *n* is the number of experiments on different cells. Electrophysiological experiments were analyzed by the Wilcoxon signed rank test. NO imaging experiments were analyzed by the Mann-Whitney *U*-test. Statistical significance was accepted at *P* < 0.05, indicated by asterisks in all figures.

Reagents. HEPES was purchased from Dojindo. DAF-2DA was from Sekisui Medical (Tokyo, Japan). *N* ω -monomethyl-L-arginine acetate (L-NMMA) and collagenase were from Wako Pure Chemicals (Osaka, Japan). Flagellin and LPS-Rhodobacter Sphaeroides (LPS-RS) were from InvivoGen (San Diego, CA). KT-5823, Rp-8-Br-cGMP, and *N*6-(1-*iminoethyl*)-L-lysine hydrochloride (L-NIL) were from Calbiochem (La Jolla, CA). A goat polyclonal anti-TLR5 blocking antibody specific to a 151–181-amino-acid residue that is a part of extracellular epitopes and is known to be one of the flagellin-binding domains (8, 15, 50) was from Enzo Life Sciences International (Farmingdale, NY). A goat-nonspecific IgG was from R&D Systems (Minneapolis, MN). A rabbit polyclonal anti-TLR5 Ab (IMG-580) specific to 300–350-amino-acid residue, which is a part of extracellular and flagellin-binding domains (7, 15), was purchased from IMGENEX and used for both the immunofluorescence and Western blotting. All other chemicals used were purchased from Sigma.

RESULTS

Potentiating effects of flagellin on ACh-induced ionic currents. We used flagellin as a ligand for TLR5. As mentioned in our previous reports (16, 17, 31, 38, 44, 45), freshly isolated tracheal submucosal gland acinar cells simultaneously generate

two kinds of [Ca²⁺]_i-dependent ionic currents under proper experimental conditions by the stimulation of ACh (30 nM). These currents are closely related to calcium oscillations, which are known to be essential for the secretory responses of many kinds of exocrine cells (5, 21, 36, 43, 46). We first investigated whether flagellin shows potentiating effects on ACh (30 nM)-induced ionic currents. As shown in Fig. 1A, 1.0 μ g/ml of flagellin significantly increased both I_o and I_i evoked by ACh (30 nM) 1.6-fold (116.4 \pm 17.0 pQ/s for ACh and 180.3 \pm 27.1 for ACh/flagellin_{1.0}, *P* < 0.05; *n* = 13) and 1.4-fold (27.9 \pm 4.2 vs. 37.0 \pm 5.4 pQ/s, *P* < 0.05; *n* = 13) of the pre-flagellin control values, respectively. When cells were stimulated by 0.5 μ g/ml of flagellin in combination with ACh (30 nM), both ACh-evoked I_o and I_i were increased 1.4-fold (164.1 \pm 40.1 pQ/s for ACh and 213.2 \pm 42.2 for ACh/flagellin_{0.5}, *P* < 0.05; *n* = 8) and 1.3-fold (28.1 \pm 8.1 vs. 37.5 \pm 10.0 pQ/s, *P* < 0.05; *n* = 8) of the pre-flagellin control values, respectively (Fig. 1B). However, 0.1 μ g/ml of flagellin showed no effect on both ACh (30 nM)-evoked I_o (169.5 \pm 40.1 pQ/s for ACh and 168.0 \pm 40.0 for ACh/flagellin_{0.1}, *P* = 0.87; *n* = 8) and I_i (14.1 \pm 3.3 vs. 14.8 \pm 3.7 pQ/s, *P* = 0.86; *n* = 8) (Fig. 1C). Flagellin (1.0 μ g/ml) per se was without effect on the baseline currents from nonstimulated resting cells (*n* = 6) (Fig. 1D). Remarkably, 1.0 μ g/ml of flagellin combined with 10 nM of ACh could generate oscillatory responses, such as those induced by 30 nM of ACh (Fig. 1E). Data summarizing the effects of flagellin on the ionic currents evoked by 30 nM of ACh are shown in Fig. 1F.

When cells were stimulated by very high concentrations (1 μ M) of ACh, they were desensitized, and flagellin no longer showed any potentiation of the ionic currents (Fig. 1G). It is suggested that flagellin can potentiate ionic currents only when the cells are moderately stimulated by low doses of ACh but not by physiologically irrelevant, robust concentrations of ACh. Intracellular calcium assays revealed that flagellin (1.0 μ g/ml) did not further increase the [Ca²⁺]_i in ACh (30 nM)-treated cells (Fig. 2). These findings suggest that flagellin potentiates the ionic responses induced by the physiologically relevant dose (30 nM) of ACh in a dose-dependent manner without any increase in [Ca²⁺]_i and that these potentiating effects would be due to the increased sensitivity of NOS to [Ca²⁺]_i signaling.

Importance of the interaction between flagellin and TLR5 in these potentiating effects. It has been reported that LPS shows the same potentiating effects as described above via the activation of TLR4 (31). To confirm the importance of the interaction between flagellin and TLR5 but not TLR4, we investigated the effects of an anti-TLR5 blocking antibody and a specific TLR4 antagonist. When cells were pretreated with 10 μ g/ml of goat anti-human TLR5 blocking antibody (anti-TLR5 Ab), the potentiating effects by flagellin on both the ACh (30 nM)-evoked I_o (169.5 \pm 41.0 pQ/s for ACh/antiTLR5Ab and 175.8 \pm 39.8 for ACh/antiTLR5Ab/flagellin, *P* = 0.34; *n* = 8) and I_i (28.1 \pm 6.9 pQ/s vs. 32.0 \pm 8.3, *P* = 0.08; *n* = 8) were completely abolished (Fig. 3A). Goat-nonspecific IgG (10 μ g/ml) did not have any inhibitory effects on the flagellin-induced potentiations (I_o: 126.0 \pm 33.2 pQ/s for ACh and 171.9 \pm 43.0 for ACh/flagellin, *P* < 0.05; *n* = 6, I_i: 29.2 \pm 5.0 vs. 38.5 \pm 6.1 pQ/s, *P* < 0.05; *n* = 6) (Fig. 3B). When cells were pretreated with LPS-RS (10 μ g/ml), a specific TLR4

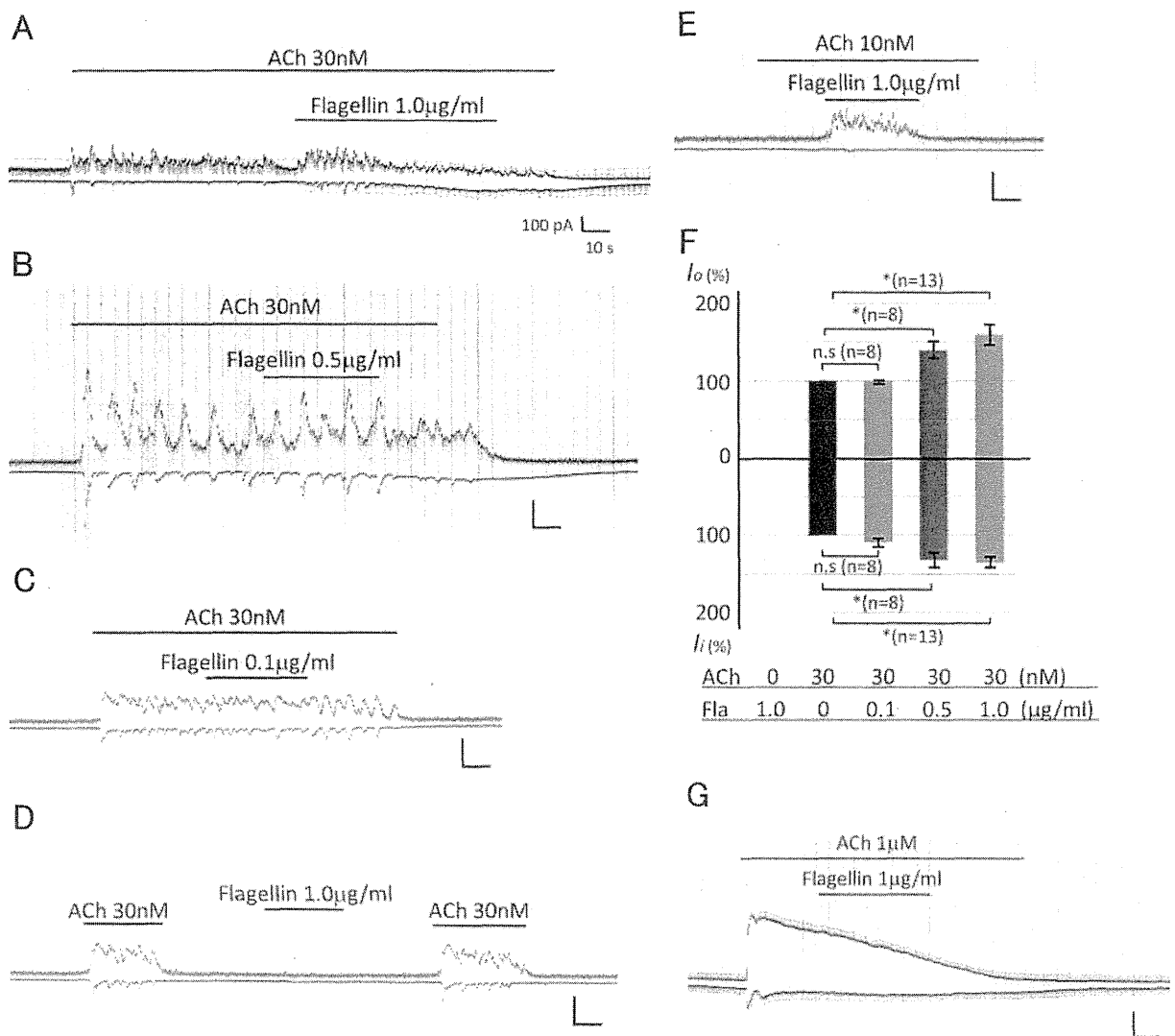


Fig. 1. Representative original recordings showing the effects of flagellin on acetylcholine (ACh) (30 nM)-evoked ionic currents. The upward or downward deflection of the current tracing represents outward current (I_o) or inward current (I_i), respectively. Using appropriate channel inhibitors and ion substitution experiments, we demonstrated that the ACh-induced I_o and I_i were carried mainly by K^+ and Cl^- , respectively, and were dependent on $[Ca^{2+}]_i$. Moreover, we found that physiologically relevant, basic secretions from swine tracheal submucosal glands could be triggered by ~30 nM of ACh (16, 17, 31, 38, 39, 44, 45). The viability of all tested cells was confirmed by the occurrence of ionic responses after the subsequent addition of 30 nM of ACh. A: 1.0 μg/ml of flagellin rapidly and significantly increased ACh (30 nM)-evoked I_o and I_i . B: 0.5 μg/ml of flagellin slightly but significantly increased ACh (30 nM)-evoked I_o and I_i . C: 0.1 μg/ml of flagellin did not cause any effects on either ACh (30 nM)-evoked I_o or I_i . D: flagellin (1.0 μg/ml) per se did not cause appreciable effects on the baseline currents in submucosal gland cells, whose viability was confirmed by the response to the subsequent addition of ACh (30 nM). E: 1.0 μg/ml of flagellin generated oscillatory responses even under the presence of as low as 10 nM of ACh, which appeared to be insufficient to generate ionic channels. F: summary of the potentiating effects of flagellin on ACh (30 nM)-evoked I_o and I_i . The electric charge movements of 20-s duration just before and after the introducing flagellin were compared by estimating the mean values of the ACh responses as 100% to exclude artifacts from differences in the membrane capacitance in each cell. Flagellin potentiated the ACh-evoked ionic currents in a dose-dependent manner, and these potentiating effects were significant only in the cases with 0.5 μg/ml of flagellin or more. * $P < 0.05$. G: robust stimulation by as high as 1 μM of ACh generated large and transient currents. However, even in the presence of ACh (1 μM), these currents were spontaneously decreased, which is known as desensitization (data not shown). In the same condition, flagellin no longer showed potentiating effects on these large currents.

antagonist, flagellin still showed a significant potentiating effect on both ACh (30 nM)-evoked I_o and I_i to 1.5-fold (101.8 ± 24.8 pQ/s for ACh and 141.1 ± 29.1 for ACh/flagellin, $P < 0.05$; $n = 7$) and 1.3-fold (12.5 ± 2.7 vs. 17.9 ± 4.8 pQ/s, $P < 0.05$; $n = 7$), respectively (Fig. 3C). Conversely, anti-TLR5 Ab did not have any inhibitory effects on the LPS-induced potentiations (I_o : 89.8 ± 17.7 pQ/s for ACh and 143.0 ± 25.5 for ACh/LPS, $P < 0.05$; $n = 8$, I_i : 25.0 ± 2.0 vs. 35.2 ± 2.3 pQ/s, $P < 0.05$; $n = 8$) (Fig. 3D). As summarized in Fig. 3E, the

maneuvers to block the interaction between flagellin and TLR5 completely abolished the potentiating effects of flagellin on the ACh (30 nM)-evoked ionic currents. Flagellin-induced potentiations were not inhibited by LPS-RS, and LPS-induced potentiations were not inhibited by anti-TLR5 Ab (Fig. 3F). These findings suggest that the interaction between flagellin and TLR5 is essential for the potentiating effects described above and that cross reactions between flagellin and TLR4 were not involved in these potentiations.

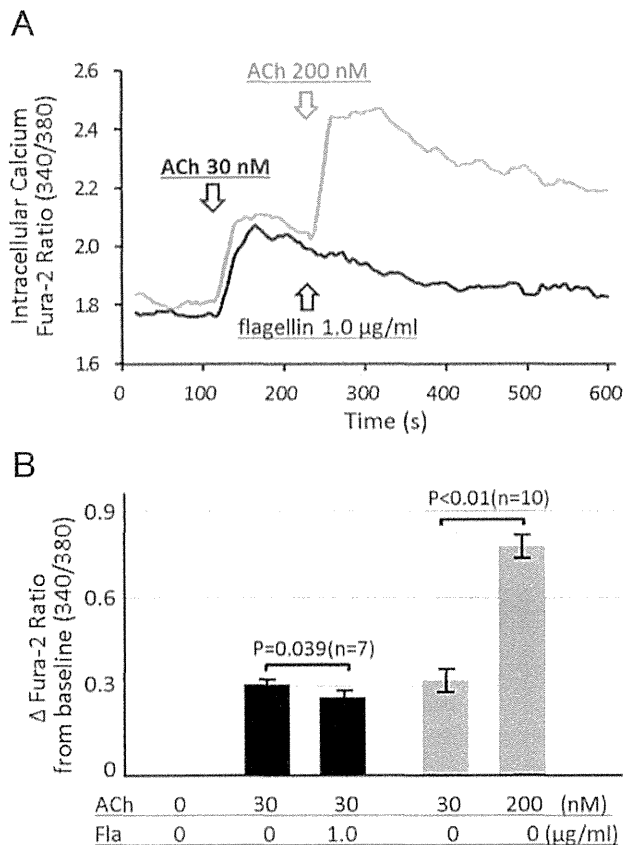


Fig. 2. Intracellular calcium assays showing no impact of flagellin on ACh (30 nM)-treated submucosal gland cells. *A*: representative tracing showing the intracellular Ca^{2+} concentration ($[\text{Ca}^{2+}]_i$) stimulated by 30 nM of ACh, followed by the subsequent addition of 1.0 $\mu\text{g}/\text{ml}$ of flagellin (black line) and 200 nM of ACh (gray line) in Fura-2-loaded tracheal submucosal gland cells. Fluorescence intensities slightly increased by 30 nM of ACh, similar to the ionic responses observed in Fig. 1. Flagellin (1.0 $\mu\text{g}/\text{ml}$) did not further increase the $[\text{Ca}^{2+}]_i$ in these cells although the cells had the capacity to increase in $[\text{Ca}^{2+}]_i$ after the stimulation by 200 nM of ACh. *B*: summary of the changes in fluorescence intensities from baseline 340/380 ratio. Baseline values (ACh 0, Fla 0) were determined by 8 data points measured over 30 s before ACh (30 nM) stimulation. Each bar represents the mean value determined by 8 data points measured over 30 s after the addition of several agonists as indicated in the bottom of graph.

Abundant expression of TLR5 on swine tracheal submucosal glands. Immunofluorescent staining and RT-PCR experiments were performed using swine tracheal specimens to confirm the expression of TLR5. As a positive control, the specimen of swine spleen was evaluated in the same way. In the immunofluorescent experiments, strong red-positive fluorescence was observed in tracheal submucosal gland cells as well as ciliated epithelial cells located on the surface of trachea (Fig. 4, *A–D*). RT-PCR also revealed a clear band corresponding to TLR5 in the product from cDNA of swine tracheal submucosal gland acinar cells (Fig. 4*E*). Western blotting analysis further confirmed the expression of TLR5 in swine tracheal submucosal gland cells (Fig. 4*F*). These findings indicate that TLR5 is certainly expressed on tracheal gland acinar cells at both the protein and mRNA levels.

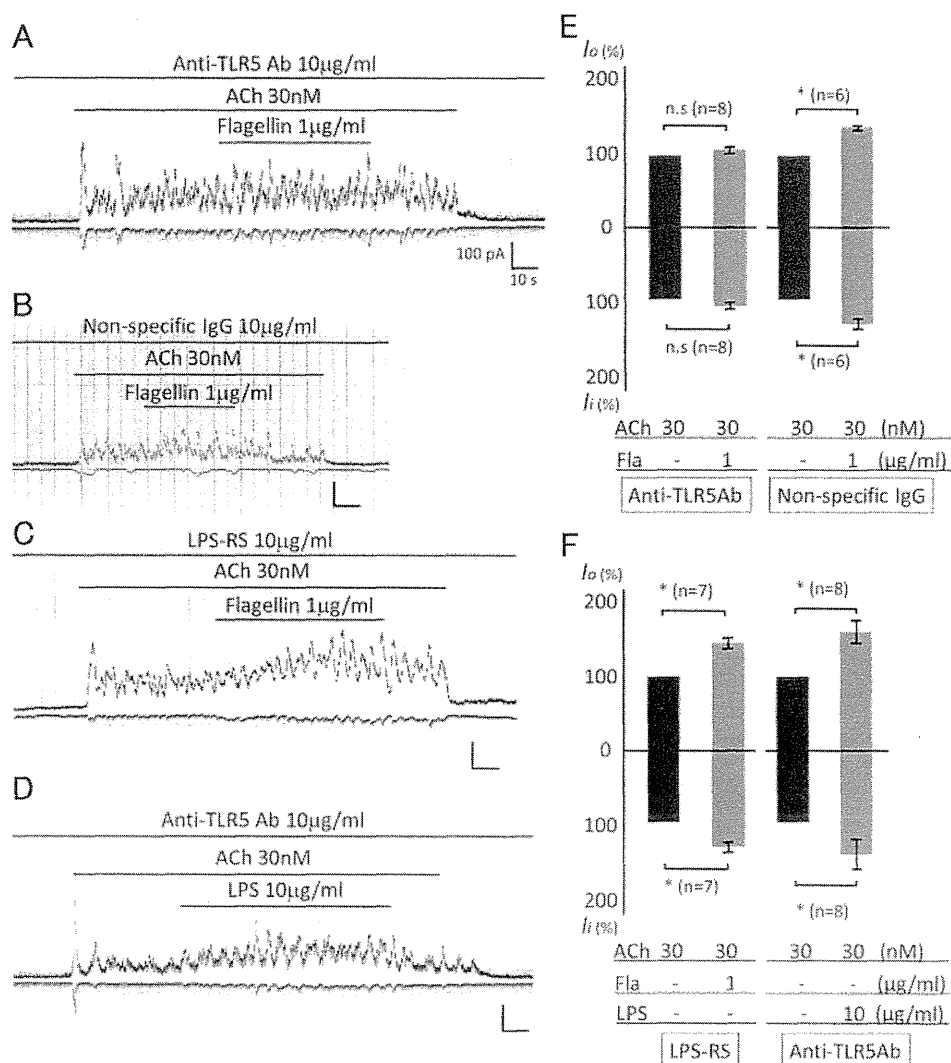
Mechanisms underlying the flagellin-induced potentiation of triggered ionic currents in submucosal gland. A relationship between flagellin/TLR5 and NO/cGMP/cGK signaling has

been suggested in some reports (26, 30). Additionally, we have also reported that LPS-induced rapid activation of TLR4 involved NO/cGMP/cGK signaling (31). Therefore, we investigated whether NO/cGMP/cGK signaling was involved in the present flagellin-induced potentiation. We used two different nonspecific NOS inhibitors, nitro-L-arginine methyl ester (L-NAME) and L-NMMA. In the presence of L-NAME (1 mM), flagellin did not show any potentiating effects on either the ACh (30 nM)-evoked I_o (172.3 ± 43.0 pQ/s for ACh/L-NAME and 167.0 ± 42.1 for ACh/L-NAME/flagellin, $P = 0.61$; $n = 7$) or I_i (37.5 ± 10.9 vs. 42.0 ± 12.3 pQ/s, $P = 0.17$; $n = 7$) (Fig. 5*A*). L-NMMA (1 mM) also completely abolished the flagellin-induced potentiating effects on both the ACh (30 nM)-evoked I_o (112.5 ± 25.2 pQ/s for ACh/L-NMMA and 108.3 ± 22.2 for ACh/L-NMMA/flagellin, $P = 0.42$; $n = 6$) and I_i (20.8 ± 8.8 vs. 24.0 ± 10.9 pQ/s, $P = 0.85$; $n = 6$) (Fig. 5*B*). Concerning the involvement of inducible NOS (iNOS), we investigated the effect of the iNOS inhibitor L-NIL. Even when cells were pretreated with L-NIL (40 μM), flagellin rather significantly increased both the ACh (30 nM)-evoked I_o (128.1 ± 42.4 pQ/s for ACh/L-NIL and 160.4 ± 40.3 for ACh/L-NIL/flagellin, $P < 0.05$; $n = 6$) and I_i (45.8 ± 11.9 vs. 52.1 ± 10.8 pQ/s, $P < 0.05$; $n = 6$) (Fig. 5*C*). As summarized in Fig. 5*F*, nonspecific NOS inhibitors completely abolished the flagellin-induced potentiating effects, but the iNOS inhibitor did not. These findings suggest that constitutive NOS, not iNOS, is involved in the TLR5-mediated rapid potentiating effects on the tracheal gland secretion.

We next investigated the involvement of cGK by using two different types of cGK inhibitors, KT-5823 and Rp-8-Br-cGMP. Under the pretreatment with 1 μM of KT-5823, flagellin did not show any potentiating effect on either the ACh (30 nM)-evoked I_o (84.4 ± 21.6 pQ/s for ACh/KT5823 and 97.9 ± 24.5 for ACh/KT5823/flagellin, $P = 0.09$; $n = 6$) or I_i (15.6 ± 5.3 vs. 17.7 ± 7.1 pQ/s, $P = 0.37$; $n = 6$) (Fig. 5*D*). Rp-8-Br-cGMP (5 μM) also completely abolished the potentiating effect by flagellin on both the ACh (30 nM)-evoked I_o (50.9 ± 11.7 pQ/s for ACh/Rp8BrcGMP and 57.1 ± 14.1 for ACh/Rp8BrcGMP/flagellin, $P = 0.09$; $n = 7$) and I_i (14.3 ± 4.5 vs. 15.1 ± 5.7 pQ/s, $P = 0.34$; $n = 7$) (Fig. 5*E*). As summarized in Fig. 5*G*, cGK inhibitors completely abolished the potentiating effects by flagellin. These findings suggest that the TLR5 ligand-mediated potentiation of triggered ionic currents in tracheal submucosal gland is closely related to the activation of NO/cGMP/cGK pathway.

Further upregulation in intracellular NO synthesis by flagellin on ACh-treated cells. To address the possibility that flagellin activates TLR5, upregulates intracellular NO synthesis, and potentiates the ACh-triggered ionic currents, we investigated whether flagellin has the ability to upregulate the synthesis of NO in tracheal gland cells. The intracellular NO synthesis was estimated using DAF-2DA, a highly specific fluorescent NO indicator as described in our previous reports (31, 44). Representative fluorescence micrographs of tracheal gland acini are shown in Fig. 6, *A–E*. Unstimulated control cells did not show any increases in the green fluorescence signals during the 40-min observation (Fig. 6*A*). On the other hand, cells stimulated by ACh (30 nM) showed slightly increased fluorescence intensities (Fig. 6*B*). Flagellin (1.0 $\mu\text{g}/\text{ml}$) in combination with ACh (30 nM) caused significantly stronger increases in the fluorescence intensities than ACh (30 nM) alone (Fig. 6*C*).

Fig. 3. Representative original recordings showing the importance of the interaction between flagellin and Toll-like receptor 5 (TLR5) in these potentiating effects. *A*: when cells were pretreated with anti-TLR5 Ab (10 $\mu\text{g}/\text{ml}$) for 1 h at 37°C, the potentiating effects of flagellin on ACh (30 nM)-evoked I_o and I_i were completely abolished. *B*: however, pretreatment with nonspecific IgG (10 $\mu\text{g}/\text{ml}$) for 1 h at 37°C did not cause any inhibitory effect on the flagellin-induced potentiation of ACh (30 nM)-evoked I_o and I_i . *C*: LPS-Rhodobacter Sphaeroides (LPS-RS) (10 $\mu\text{g}/\text{ml}$), a specific TLR4 antagonist, did not disturb the potentiating effects of flagellin on ACh (30 nM)-evoked I_o and I_i . *D*: conversely, anti-TLR5 Ab did not have any inhibitory effects on the LPS-induced potentiations. *E*: summary of the effects of anti-TLR5 Ab, nonspecific IgG, and LPS-RS on the flagellin-induced potentiation to ACh (30 nM)-evoked I_o and I_i . Under the presence of anti-TLR5 Ab, flagellin did not have significant potentiating effects on the ACh-evoked I_o and I_i . However, neither nonspecific IgG nor LPS-RS influenced the potentiating effects of flagellin on ACh-evoked I_o and I_i . The specificity of anti-TLR5 Ab to block TLR5 but not TLR4 was confirmed by its lack of effect on LPS potentiations. * $P < 0.05$.



Interestingly, when cells were preincubated with 10 $\mu\text{g}/\text{ml}$ of anti-TLR5 Ab, the fluorescence intensities under the presence of both flagellin (1.0 $\mu\text{g}/\text{ml}$) and ACh (30 nM) were at almost the same levels as those under the presence of ACh (30 nM) alone (Fig. 6D). Moreover, the cells stimulated by flagellin (1.0 $\mu\text{g}/\text{ml}$) alone showed slightly increased fluorescence intensities (Fig. 6E). A summary of the changes in the time courses is shown in Fig. 6F. Fluorescence intensities were calculated by measuring the intensities per unit area from the cytosol and were compared by estimating mean intensities of prestimulation (0 min) as 1.0. Under the stimulation by flagellin (1.0 $\mu\text{g}/\text{ml}$) in combination with ACh (30 nM), the fluorescence intensities increased more rapidly and strongly than in cells stimulated by ACh alone. However, these significant increases in the fluorescence intensities were completely abolished in the presence of anti-TLR5 Ab, and these intensity curves were at almost the same levels as those stimulated by ACh (30 nM) alone. These findings are in line with electrophysiological experiments (see Fig. 1F and 3E). When the fluorescence intensities were estimated at 10 min, flagellin (1.0 $\mu\text{g}/\text{ml}$) significantly increased the ratio in intensities up to 1.2-fold compared with ACh (30 nM)-stimulated cells (1.04 ± 0.02 for ACh-stimulated value; $n = 7$, and 1.24 ± 0.04 for ACh/

flagellin-stimulated value; $n = 9$, $P < 0.05$) (Fig. 6G). These upregulations in NO syntheses were almost completely abolished under the presence of anti-TLR5 Ab (Fig. 6G). These findings suggest that interaction between flagellin and TLR5 significantly upregulates the NO synthesis, contributing to the potentiating effect on electrolytes secretion from tracheal gland cells under physiologically relevant stimulation by ACh (30 nM).

DISCUSSION

In chronic inflammatory airway diseases such as COPD, *P. aeruginosa* often colonizes the airway mucosal surface and appears to have a role in the persistent inflammation or hypersecretion in the airways that results in repeated exacerbations in these diseases (42). However, the exact reason why *P. aeruginosa* is closely related to hypersecretion is still not well understood. We considered that PAMPs might be involved. Both *P. aeruginosa* flagellin and LPS are PAMPs recognized by host pathogen-recognition receptors, TLR4 and TLR5, respectively (1). We have reported that LPS derived from *P. aeruginosa* caused significant potentiating effects on airway serous gland secretion via the activation of TLR4 (31). Be-

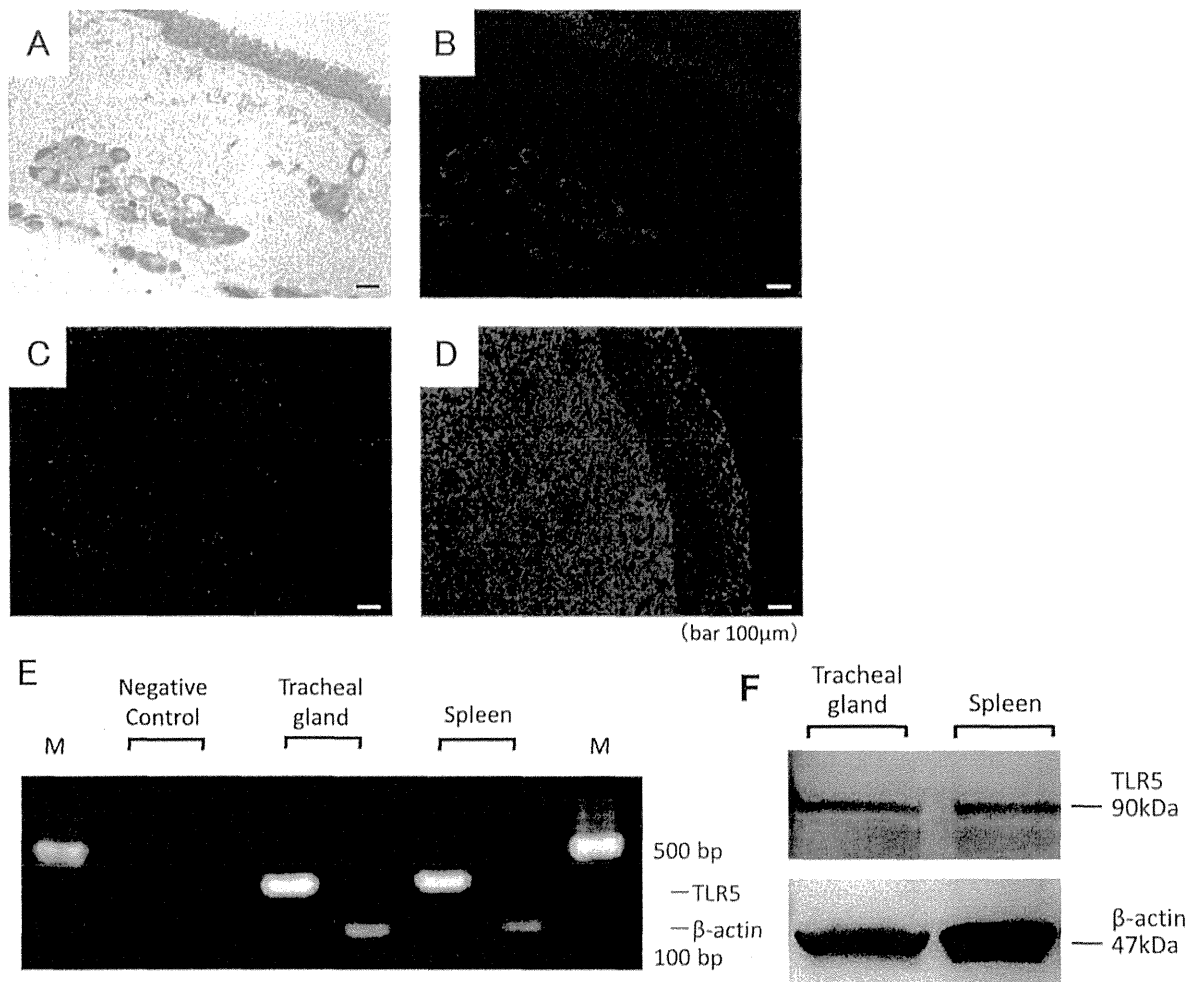


Fig. 4. Expression of TLR5 on swine tracheal submucosal gland acinar cells using immunofluorescent staining (A–D) and RT-PCR (E). Scale bars = 100 μ m. A: photomicrograph of swine trachea showed abundant, localized submucosal glands beneath the surface tracheal epithelium. B: immunofluorescent staining showed strong red signals (TLR5) from the submucosal glands as well as tracheal epithelium. C: swine trachea was counterstained with DAPI (blue). D: as a positive control tissue, a section from swine spleen was evaluated in the same way. Obvious red signals were observed on spleen tissue. E: RT-PCR also demonstrated the clear expression of TLR5-mRNA from tracheal submucosal gland acinar cells and was observed in swine spleen as a positive control tissue. Negative control by skipping the reverse transcriptional step showed no amplification. M, marker. F: Western blotting analysis revealed the expression of TLR5 protein (90 kDa) in swine tracheal submucosal gland cells. Control was extract prepared from swine spleen.

cause LPS is known to be a prototypical example of endotoxin, it might cause nonspecific effects other than as a TLR4 ligand in vivo. In the present study, we focused on the function of TLR5 as another possible potentiator of airway serous secretion. Flagellin significantly potentiated Cl^- secretion from freshly isolated tracheal submucosal gland acinar cells in a dose-dependent manner, and its potentiating effect was reproduced only when the cells were stimulated by physiologically relevant low doses of ACh (30 nM) (basal secretion) but not by robust doses of ACh (1 μ M) (experimental maximum stimulation). Flagellin significantly increased the ACh-induced intracellular NO synthesis, and NO/cGMP/cGK signaling was involved in this rapid potentiation by flagellin/TLR5. Additionally, our studies presented here showed the absence of any interaction between the flagellin/TLR5 signaling and LPS/TLR4 signaling because the flagellin-induced potentiations were not inhibited by LPS-RS and the LPS-induced potentiations were not inhibited by anti-TLR5 Ab (Fig. 3F). Combined with our previous report (31), these findings suggested that

both TLR4 and TLR5 are endogenous potentiators of serous secretion from tracheal submucosal gland acinar cells and are likely to play important roles in the pathogenesis of airway hypersecretion in chronic *P. aeruginosa* infection. Concerning the concentration of flagellin, Yu and colleagues (51) reported that flagellin (0.1–10.0 μ g/ml) upregulated MUC5AC expression by activating TLR5 on 16HBE cells, but 0.01 μ g/ml of flagellin did not (51). Illek and colleagues (14) reported that flagellin (0.1–1.0 μ g/ml) activated p38, NF- κ B, IL-8, and cystic fibrosis transmembrane conductance regulator (CFTR)-dependent airway secretion in Calu-3 cells. These reports are in line with ours. However, other reports showed that as low as 50–200 ng/ml of flagellin significantly upregulated IL-8 production and IL-23 production in airway epithelial cells (41) and intestinal dendritic cells (23), respectively. We do not have a clear explanation for these differences, but we suppose that submucosal gland cells need a relatively high concentration of flagellin to potentiate airway secretion in vitro; otherwise they need carrier proteins or something to enhance the effects of flagellin in vivo.